ARCHIVES OF ACOUSTICS
3, 3, 153-174 (1978)

THE EFFECT OF INPUT CROSS-SPECTRA ON THE ESTIMATION OF FREQUENCY RESPONSE IN CERTAIN MULTIPLE-INPUT SYSTEMS*

A. F. SEYBERT AND M. J. CROCKER

Ray W. Herrick Laboratory, School of Mechanical Engineering, Purdue University, W. Lafayette (Indiana 47907)

Department of Mechanical Engineering, University of Kentucky, Lexington (Kentucky 40506)

The estimation of frequency response of multiple input systems is discussed from the standpoint of systems identification, with application to problems in noise control. The systems considered are assumed to have inputs, either random or deterministic, that are identical in form but shifted in time. Such inputs are found typically as force and pressure excitations in engines, pumps and compressors. It is shown that the input cross-spectra can be neglected for inputs of this type, providing proper frequency smoothing is used. If the time-shift between inputs is not equal or if the analysis bandwidth cannot be chosen arbitrarily, biased estimates of the frequency responses will result when the input cross-spectra are neglected. Expressions for this bias error are developed and several numerical examples are presented showing the effect of analysis bandwidth and timeshift on the bias error. This technique was applied to the problem of estimating the structural-acoustical frequency response of a diesel engine. By neglecting the cross-spectra between the combustion pressures the frequency responses were computed on-line with a small digital processor. As a result experimental and computer time were greatly reduced.

List of symbols

B_e — bandwidth [Hz]
f — frequency [Hz]
f_i — natural frequency of the i^{th} input
H_i — frequency response to the i^{th} input
k — frequency index of unsmoothed spectrum
m — frequency index of smoothed spectrum
K — number of frequency points smoothed per band
N — number of inputs
$x_i(t)$ — i^{th} input to system
$y'(t)$ — coherent output
$y(t)$ — total output
$z(t)$ — incoherent uncorrelated output
S_{ii} — auto-spectrum of the i^{th} input
S_{ij} — cross-spectrum between the i^{th} and j^{th} inputs
S_{iy} — cross-spectrum between the i^{th} input and total output

* Presented, in part, at the 89th Meeting of the Acoustical Society of America, April 1975.

$S_{iy'}$ — cross-spectrum between the i^{th} input and coherent output
S_{iz} — cross-spectrum between the i^{th} input and incoherent output
S_{zz} — auto-spectrum of incoherent output
S_{yy} — auto-spectrum of total output
$S_{y'y'}$ — auto-spectrum of coherent output
T — record length
Z_i — gain of the i^{th} system
ξ — damping ratio
τ_i — time delay between inputs i and 1
τ_{ij} — time delay between inputs i and j
φ_{ij} — phase angle between inputs i and j
$\hat{\eta}$ — estimate of any parameter η
$E\{\hat{\eta}\}$ — expected value of $\hat{\eta}$
$b\{\hat{\eta}\}$ — bias error of $\hat{\eta}$

Introduction

In modeling dynamic systems, one often requires information to complete the model that can only be accurately known from experiment. The process of determining this information is termed "parameter identification" since the needed information is in the form of one or more unknown parameters in the mathematical model [1]. For example, a second-order model has two unknown parameters: the system natural frequency and damping.

Traditionally, controlled laboratory experiments have been used to ascertain system properties. The system to be modeled is subjected to a known artificial excitation and the response is compared to the theoretical response as predicted by the mathematical model. The unknown parameters are then selected, by predetermined criteria, to yield the best agreement between predicted and experimental system response. The experimental techniques can be either time domain (such as step or pulse response) or frequency domain. For frequency domain testing the system excitation can be in the form of sinusoidal steady state, sine sweep, impulsive, step or stationary random.

Alternatively, it is possible to determine dynamic properties while a system is in its actual operating environment. This method is attractive for studying systems not suitable for laboratory testing, e.g. ships, buildings, and other structures. Parameter identification is accomplished by studying the system response due to normally occurring excitations, providing that the excitations and response are measurable. Since, in general, these quantities will be random, stochastic theory is involved in the measurement and analysis processes. A benefit of *in situ* testing is that the unknown parameter estimates are usually more realistic than those obtained by laboratory testing since in the latter case the system is removed from its operating environment. However, for *in situ* testing the measurement and analysis techniques must remove, or properly account for, the effect of extraneous information (e.g. ambient sound and vibration).

The estimate of the frequency response of a system is a useful information in determining unknown parameters. In the system control, frequency response data aids in the formulation of control strategy. Even in uncontrolled systems (e.g. climate) the frequency response data are useful for predicting the system behavior to sets of selected inputs.

Frequency response techniques can be applied to certain acoustic systems, particularly with respect to practical problems of noise control. When the system under study is a noise source of complex geometry, such as most machinery noise sources, simple acoustical models using idealized geometries (spheres, cylinders, panels, etc.) often do not yield detailed information about the system and its behavior. Frequency response data (providing it can be obtained) can give an insight into the system behavior and aid in formulating a more realistic acoustical model.

Chung et al. [2-3] have used frequency response techniques to determine the structural-acoustical behavior of diesel engines. Chung considered the engine as a set of N linear systems with N inputs x_i, $i = 1, 2, \ldots, N$ (cylinder pressures corresponding to the combustion excitation in the N cylinders of the engine) and a single output y (the engine noise measured at a point about 1 m from the side of the engine).

The uncorrelated output z is included in the model to account for any extraneous effects such as ambient sound or instrumentation noise. The frequency responses were calculated from measured time records of the system inputs and outputs using multiple input linear theory [4].

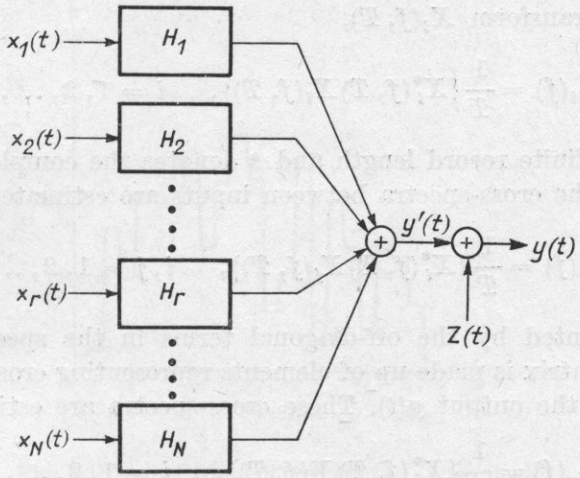

Fig. 1. A multiple input system with uncorrelated output z

Seybert and Crocker [5-6] used the diesel engine frequency responses to predict the effect on noise of engine operating conditions such as speed, load and injection timing.

The frequency responses are calculated by solving the following set of algebraic equations, utilizing spectral estimates computed from measured time records [4], where it is assumed that the time records are stationary:

$$[S_{iy}(f)] = [S_{ij}(f)][H_i(f)], \tag{1}$$

where the frequency response matrix

$$[H_i(f)] = \begin{bmatrix} H_1(f) \\ H_2(f) \\ \cdots \\ H_N(f) \end{bmatrix},$$

the spectral matrix

$$[S_{ij}(f)] = \begin{bmatrix} S_{11}(f) & S_{12}(f) \ldots S_{1N}(f) \\ S_{21}(f) & S_{22}(f) \ldots S_{2N}(f) \\ \cdots\cdots\cdots\cdots\cdots \\ S_{N1}(f) & S_{N2}(f) \ldots S_{NN}(f) \end{bmatrix},$$

the cross-spectral matrix

$$[S_{iy}(f)] = \begin{bmatrix} S_{1y}(f) \\ S_{2y}(f) \\ \cdots \\ S_{Ny}(f) \end{bmatrix}.$$

The diagonal elements of the spectral matrix are the auto-spectral densities of each input $x_i(t)$. These spectra can be estimated from computations of the finite Fourier transform $X_i(f, T)$,

$$\hat{S}_{ii}(f) = \frac{1}{T}\{X_i^*(f, T) X_i(f, T)\}, \quad i = 1, 2, \ldots, N, \tag{2}$$

where T is the finite record length and * denotes the complex conjugate.

Similarly, the cross-spectra between inputs are estimated by

$$\hat{S}_{ij}(f) = \frac{1}{T}\{X_i^*(f, T) X_j(f, T)\}, \quad i, j = 1, 2, \ldots, N \tag{3}$$

and are represented by the off-diagonal terms in the spectral matrix. The cross-spectral matrix is made up of elements representing cross-spectra between each input and the output $y(t)$. These cross-spectra are estimated by

$$\hat{S}_{iy}(f) = \frac{1}{T}\{X_i^*(f, T) Y(f, T)\}, \quad i = 1, 2, \ldots, N. \tag{4}$$

It should be noted that the spectral estimates computed by using equations (2)-(4) are inconsistent estimates and some form of smoothing must be used to reduce the variance of the estimates. Smoothing also removes the effect of the extraneous output $z(t)$, providing it is uncorrelated with respect to all inputs ($S_{iz}(f) = 0$, $i = 1, 2, \ldots, N$). If this is true, then it can be shown [4] that

$$S_{iy}(f) = S_{iy'}(f), \quad i = 1, 2, \ldots, N,$$

where $S_{iy'}(f)$ is the cross-spectrum between each input and the coherent output $y(t)$.

Using the quantities defined above, the total output spectral density $S_{yy}(f)$ can be computed by

$$S_{y'y'}(f) = S_{zz}(f) + S_{yy}(f), \tag{5}$$

where $S_{zz}(f)$ is the spectral density of the uncorrelated output $z(t)$, and

$$S_{y'y'}(f) = \sum_{i=1}^{N} \sum_{j=1}^{N} S_{ij}(f) H_i^*(f) H_j(f) \tag{6}$$

is the spectral density of the coherent output $y'(t)$.

A typical frequency response for the diesel engine is shown [5] in Fig. 2. It was computed using equation (1) with measured time records for the combustion pressures (measured by quartz pressure transducers in each cylinder) and the sound pressure as measured by a condenser microphone located about 1 m from the side of the engine. The engine was operating in a free-field environment. The frequency response in Fig. 2 describes the structural-acoustical behavior of the combustion induced noise; regions where the frequency response is high correspond to high dynamic response and/or high radiation efficiency of the engine structure.

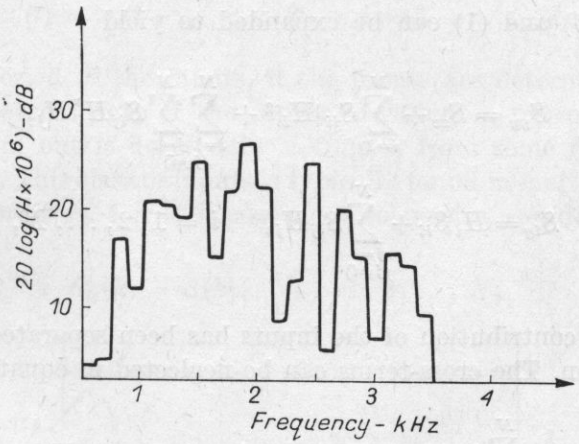

Fig. 2. Typical frequency response (magnitude) for one cylinder of a diesel engine

A problem associated with estimating the frequency responses of multiple input systems is the large number of cross-spectra between inputs that must be estimated for equation (1). For an N input system, $N(N-1)/2$ input cross-spectra must be estimated (the divisor 2 appears since the lower triangle cross-spectra in the spectral matrix are computed from the complex conjugate of the upper triangle spectra – $S_{ij}(f) = S_{ji}^*(f)$ – see equation (3)). Since the total number of spectral estimates needed for equation (1) is $N(N+3)/2$, the input cross-spectra represent a fraction of $(N-1)/(N-3)$ of the total spectra.

Many analog-to-digital converters and digital processors do not have sufficient capability to sample and compute more than one cross-spectral estimate at a time, thus making experimental time quite long for systems with many inputs. In addition, most mini-computer systems cannot perform matrix inversion (necessary to solve equation (1)) for large values of N due to computer core limitations.

The remainder of this paper will discuss a class of inputs normally occurring in many physical systems, where the input cross-spectra can be neglected. With such systems experimental time is reduced and the frequency responses can be computed from a set of uncoupled equations (1) (with input cross-spectra neglected). The computations are then suitable for mini-computers with small memories since matrix inversion is unnecessary. That is, equation (1) reduces to a set of equations

$$H_i(f) = S_{iy}(f)/S_{ii}(f), \quad i = 1, 2, \ldots, N. \tag{7}$$

Conditions for neglecting cross-spectral terms

Equations (5) and (1) can be expanded to yield

$$S_{yy} = S_{zz} + \sum_{i=1}^{N} S_{ii}|H_i|^2 + \sum_{\substack{i=1 \\ (j\neq i)}}^{N}\sum_{j=1}^{N} S_{ij}H_i^* H_j, \tag{8}$$

$$S_{iy} = H_i S_{ii} + \sum_{\substack{j=1 \\ (j\neq i)}}^{N} S_{ij}H_j, \quad i = 1, 2, \ldots, N, \tag{9}$$

where the direct contribution of the inputs has been separated from the cross--term contribution. The cross-terms can be neglected in equation (9) providing

$$\sum_{\substack{j=1 \\ (j\neq i)}}^{N} S_{ij}H_j \ll H_i S_{ii}, \quad i = 1, 2, \ldots, N, \tag{10}$$

or

$$\sum_{\substack{j=1 \\ (j\neq i)}}^{N} S_{ij}H_i^* H_j \ll |H_i|^2 S_{ii}, \quad i = 1, 2, \ldots, N,$$

thus

$$\sum_{i=1}^{N}\sum_{\substack{j=1 \\ (j\neq i)}}^{N} S_{ij}H_i^* H_j \ll \sum_{i=1}^{N} S_{ii}|H_i|^2. \tag{11}$$

Hence, if equation (10) can be established, then equation (11) follows and equations (8) and (9) reduce to

$$S_{yy} = S_{zz} + \sum_{i=1}^{N} S_{ii} |H_i|^2, \tag{12}$$

$$S_{iy} = H_i S_{ii}. \tag{13}$$

There are several conditions under which equation (10) is fulfilled, however, most are trivial. For example, if the inputs are independent random processes so that $S_{ij} = 0$ for $i \neq j$ or if one-frequency response is dominant, see equation (9) (in which case the multiple input system reduces to a single input system), equation (10) is satisfied. There may also be certain symmetries between the frequency responses that would satisfy equation (10), but in general this will not be the case. In the case of the diesel engine, symmetry does exist between the arrangement of the cylinders and the microphone position, but measurements of the frequency responses do not reflect this.

One general condition that satisfies equation (10) occurs when the inputs are of the form

$$x_i(t) = x_1(t+\tau_i), \tau_i < T, \quad i = 1, 2, \ldots, N, \tag{14}$$

where T is the period of the inputs, if the inputs are deterministic processes, or the sample record length if the inputs are random processes. Each input has the same form but is delayed by a time τ_i from some reference (here *1*) input, as in Fig. 3. This class of inputs is typically found in multicylinder engines, pumps, and compressors. For this case the auto-spectra are identical (see equation (2)),

$$S_{ii}(k) = S(k), \quad i = 1, 2, \ldots, N, \tag{15}$$

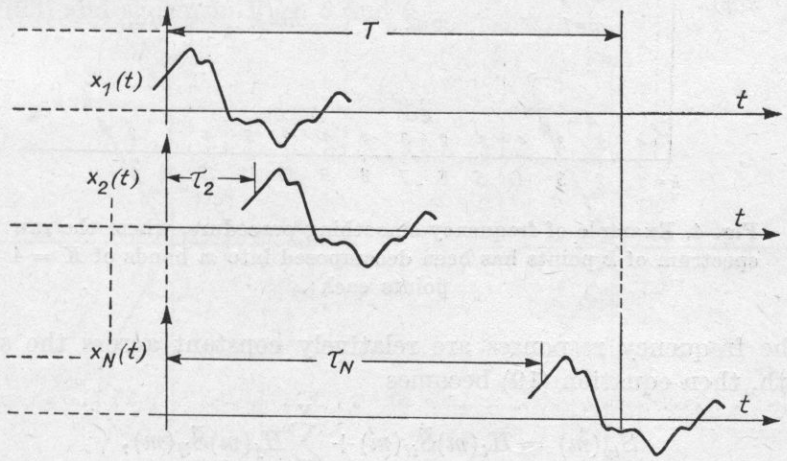

Fig. 3. Identical inputs except delayed in time

and the cross-spectra are given by (see equation (3))

$$S_{ij}(k) = S(k)e^{i\varphi ij(k)}, \quad j \neq i;\ i,j = 1,2,\ldots,N, \tag{16}$$

where

$$\varphi_{ij}(k) = \frac{\tau_{ij}(2\pi k)}{T}, \quad \tau_{ij} = \tau_i - \tau_j, \tag{17}$$

and $k = 1, 2, \ldots$ is the harmonic multiple of the fundamental frequency $1/T$.

Frequency smoothing is often used to reduce the variance of a spectral estimate and is accomplished by averaging the spectral values of the raw spectrum over a selected bandwidth. The disadvantage is a loss of frequency resolution since the bandwidth is increased from $1/T$ to K/T, where K is the number of spectral values averaged. That is, a smoothed spectrum is given by

$$\bar{S}(m) = \frac{1}{K}\sum_{l=1}^{K} S(l,m), \tag{18}$$

where the raw spectra $S(k)$ of k points have been decomposed into m bands of K points each (Fig. 4). Smoothing equation (9) yields

$$S_{iy}(m) = \frac{1}{K}\sum_{l=1}^{K} S_{iy}(l,m) = \frac{1}{K}\sum_{l=1}^{K}\left\{H_i(l,m)S_{ii}(l,m) + \sum_{\substack{j=1\\(j\neq i)}}^{N} S_{ij}(l,m)H_j(l,m)\right\}. \tag{19}$$

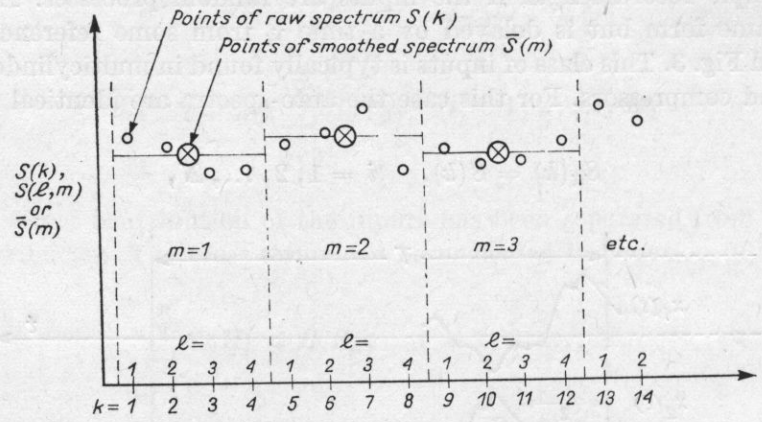

Fig. 4. Example of frequency smoothing procedure, where the raw spectrum of k points has been decomposed into m bands of $K = 4$ points each

If the frequency responses are relatively constant across the smoothing bandwidth, then equation (19) becomes

$$\bar{S}_{iy}(m) = H_i(m)\bar{S}_{ii}(m) + \sum_{\substack{j=1\\(j\neq i)}}^{N} H_j(m)\bar{S}_{ij}(m), \tag{20}$$

where

$$\bar{S}_{ii}(m) = \frac{1}{K}\sum_{l=1}^{K} S_{ii}(l, m) \quad \text{and} \quad \bar{S}_{ij}(m) = \frac{1}{K}\sum_{l=1}^{K} S_{ij}(l, m).$$

Examining $\bar{S}_{ij}(m)$ for the inputs described by (14) we get

$$\bar{S}_{ij}(m) = \frac{1}{K}\sum_{l=1}^{K} S(l, m)\, e^{i\varphi_{ij}(k)}. \tag{21}$$

If the auto-spectrum of the inputs $S(l, m)$ is relatively constant across the smoothing bandwidth, then

$$\bar{S}_{ij}(m) = \frac{S(m)}{K}\sum_{l=1}^{K} e^{i\varphi_{ij}(l,m)}. \tag{22}$$

It can be shown mathematically that

$$\sum_{l=1}^{K} e^{i\varphi_{ij}(l,m)} = 0, \quad j \neq i;\ i, j = 1, 2, \ldots, N. \tag{23}$$

For the case where the time delay between any two consecutively numbered inputs is T/N we have

$$\tau_{ij} = \frac{(i-j)T}{N}. \tag{24}$$

For this case equation (20) gives

$$\bar{S}_{iy}(m) = H_i(m)\,\bar{S}_{ii}(m), \quad i = 1, 2, \ldots, N. \tag{25}$$

In equation (23) the quantity $e^{i\varphi_{ij}(l,m)}$ can be interpreted as the "roots of unity" and represented geometrically in Figs. 5 and 6 for $N = 3$ and $N = 6$, respectively. An interesting property of these roots is that for any specified values N and $i-j$ the sum of the corresponding roots is zero, a fact stated in equation (23) and shown in Figs. 5 and 6.

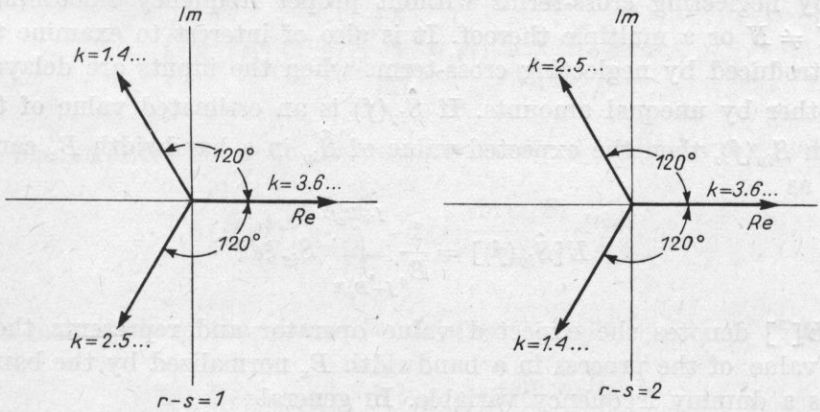

Fig. 5. Example of the function $e^{i\varphi_{ij}k}$ for different values of $i-j$ for $N = 3$

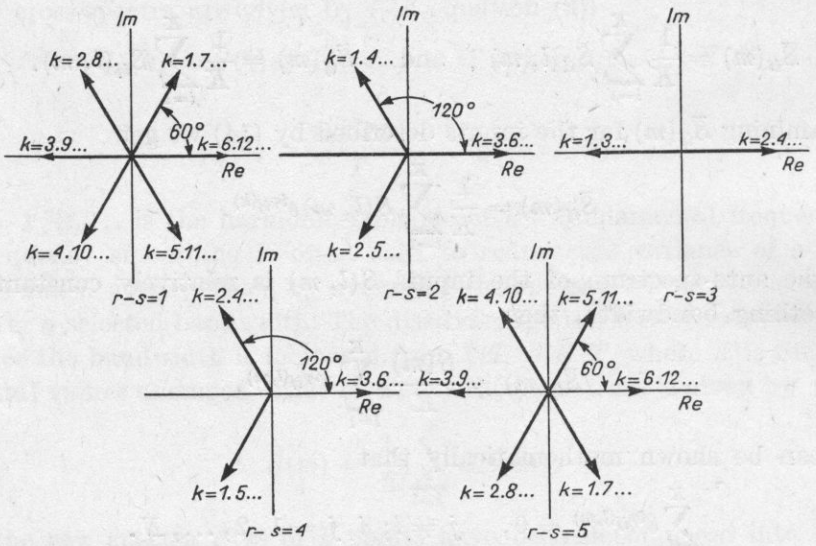

Fig. 6. Example of the function $e^{i\varphi_{ijk}}$ for different values of $i-j$ for $N = 6$

Consequently, there exists an optimum smoothing index K, equal to the number of mutually coherent inputs N, or a multiple thereof, that will allow the cross-spectral terms between inputs to be ignored in calculating frequency responses and in predicting the system output, when the inputs are given by equation (14).

Bias errors

In many practical cases one cannot restrict the analysis bandwidth to a multiple of N harmonics necessary to establish equation (25) or the time delay may not be as in equation (24). The question arises: "What bias error is introduced by neglecting cross-terms without proper frequency smoothing," i.e., when $K \neq N$ or a multiple thereof. It is also of interest to examine the bias error introduced by neglecting cross-terms when the inputs are delayed from one another by unequal amounts. If $\hat{S}_{iy}(f)$ is an estimated value of the true spectrum $S_{iy}(f)$, then the expected value of $\hat{S}_{iy}$ in a bandwidth B_e can be expressed as

$$E[\hat{S}_{iy}(f)] = \frac{1}{B_e} \int_{f-B_e/2}^{f+B_e/2} S_{iy}\,\xi d\xi \tag{26}$$

where $E[\ ]$ denotes the expected value operator and represents the mean-square value of the process in a bandwidth B_e normalized by the bandwidth, and ξ is a dummy frequency variable. In general

$$E[\hat{S}_{iy}(f)] \neq S_{iy}(f)$$

due to bias errors associated with the form of the actual spectrum S_{iy} or the nature of the estimation process. The bias error $b[\hat{S}_{iy}(f)]$ is defined as

$$b[\hat{S}_{iy}(f)] = E[\hat{S}_{iy}(f) - S_{iy}(f)]. \tag{27}$$

Stationary random inputs

Using equations (9), (15), (16) and (26) one obtaines

$$E[\hat{S}_{iy}(f)] = \frac{1}{B_e} \int_{f-B_e/2}^{f+B_e/2} \left\{ H_i(\xi) S(\xi) + S(\xi) \sum_{\substack{j=1 \\ (j \neq i)}}^{N} H_j(\xi) e^{i\varphi_{ij}(\xi)} \right\} d\xi \quad i = 1, 2, \ldots, N, \tag{28}$$

where the spectral quantities have been expressed as continuous functions of frequency rather than discrete values at harmonic numbers k.

Also

$$\varphi_{ij} = 2\pi f \tau_{ij}, \tag{29}$$

where τ_{ij} is the delay between any two inputs i and j.

If $S(f)H_j(f)$ $(j = 1, 2, \ldots, N)$ is not a strong function of frequency across the smoothing bandwidth B_e, then equation (28) becomes

$$E[\hat{S}_{ij}(f)] = H_i(f)S(f) + \frac{1}{B_e} \sum_{\substack{j=1 \\ (j \neq i)}}^{N} S(f) H_j(f) \int_{f-B_e/2}^{f+B_e/2} e^{i\varphi_{ij}(\xi)} d\xi$$

or

$$E[\hat{S}_{iy}(f)] = S(f) \left\{ H_i(f) + \sum_{\substack{j=1 \\ (j \neq i)}}^{N} H_j(f) \frac{\sin \psi_{ij} B_e}{\psi_{ij} B_e} e^{i2\psi_{ij} f} \right\}, \tag{30}$$

where $\psi_{ij} = \pi \tau_{ij}$. Therefore the bias error in $\hat{S}_{iy}(f)$ is, from equation (27),

$$b[S_{iy}(f)] = S(f) \sum_{\substack{j=1 \\ (j \neq i)}}^{N} H_j(f) \frac{\sin \psi_{ij} B_e}{\psi_{ij} B_e} e^{i2\psi_{ij} f}, \tag{31}$$

and the bias error for the frequency response (defined similarly to equation (27))

$$b[\hat{H}_i(f)] = \sum_{\substack{j=1 \\ (j \neq i)}}^{N} H_j(f) \frac{\sin \psi_{ij} B_e}{\psi_{ij} B_e} e^{i2\psi_{ij} f}. \tag{32}$$

The magnitude of the bias of the frequency response can be expressed as

$$|b[H_i(f)]| \leqslant \sum_{\substack{j=1 \\ (j \neq i)}}^{N} |H_j(f)| \left| \frac{\sin \psi_{ij} B_e}{\psi_{ij} B_e} \right|, \tag{33}$$

so that the equality in equation (33) is the upper bound of the bias error for the frequency response magnitude. The zeros of equations (31)-(33) occur if

$$\frac{\sin \psi_{ij} B_e}{\psi_{ij} B_e} = 0,$$

that is

$$\psi_{ij} B_e = n\pi, \quad n = 1, 2, ..,$$

or, using the definition of ψ_{ij},

$$B_e = \frac{n}{\tau_{ij}}, \quad j \neq i;\ i, j = 1, 2, \ldots, N. \tag{34}$$

Therefore, in general, there is no bandwidth that will result in zero bias error for all of the inputs under consideration. One exception is when the time delays are given by equation (24), in which case the largest bandwidth is

$$B_e = \frac{nN}{T}, \tag{35}$$

which is in agreement with the interpretation of equation (23). Although a special case, many physical systems have inputs of this form. In general though, an optimum bandwidth would be selected that would minimize the bias errors for all the frequency responses according to some predetermined criterion — for example that the sum of the bias errors for all the frequency responses should be a minimum.

Bias errors — periodic inputs

In the case of periodic inputs of the form of equation (14), where T is the period of the inputs, the bandwidth is restricted to a multiple of $1/T$, the fundamental frequency of the inputs. In this case, the expected value of the cross-spectrum between each input and the output is

$$E[\hat{S}_{iy}(m)] = \frac{1}{K} \sum_{l=1}^{K} S_{iy}(l, m), \tag{36}$$

and the bias error

$$b[\hat{S}_{iy}(m)] = E[\hat{S}_{iy}(m) - \hat{S}_{iy}(m)]. \tag{37}$$

Substituting equations (9) and (15) into (36) we get

$$E[\hat{S}_{iy}(m)] = \frac{1}{K} \sum_{l=1}^{K} H_i(l, m) S(l, m) + S(l, m) \sum_{\substack{j=1 \\ (j \neq i)}}^{N} H_j(l, m) e^{i\varphi_{ij}(l,m)}$$
$$(i = 1, 2, \ldots, N). \tag{38}$$

Again, assuming that the spectra and frequency responses are not highly variable across any band K/T, we have

$$E[\hat{S}_{iy}(m)] = S(m)\left\{H_i(m) + \sum_{\substack{j=1\\(j\neq i)}}^{N} H_j(m)\frac{1}{K}\sum_{l=1}^{K} e^{i\varphi_{ij}(l,m)}\right\}.$$

Since

$$E[\hat{S}_{iy}(m)] = S(m)\left\{H_i(m) + \sum_{\substack{j=1\\(j\neq i)}}^{N} H_j(m)\frac{e^{i2\pi\tau_{ij}Km/T}}{K}\left[\left(-\frac{1}{2} + \frac{\sin[(K+\frac{1}{2})\tau_{ij}2\pi/T]}{2\sin(\tau_{ij}\pi/T)}\right) + \right.\right.$$

$$\left.\left. + i\left(\frac{1}{2}\cot\frac{\tau_{ij}\pi}{T} - \frac{\cos(K+\frac{1}{2})\tau_{ij}2\pi/T}{2\sin(\tau_{ij}\pi/T)}\right)\right]\right\},$$

the bias of the frequency response is

$$b[\hat{H}_i(m)] = \sum_{\substack{j=1\\(j\neq i)}}^{N} \frac{H_j(m)\,e^{i2\varphi_{ij}Km/T}}{2K}\left[\left(-1 + \frac{\sin[(K+\frac{1}{2})2\psi_{ij}/T]}{\sin(\psi_{ij}/T)} + \right.\right.$$

$$\left.\left. + i(\cot\psi_{ij}/T) - \frac{\cos[(K+\frac{1}{2})2\psi_{ij}/T]}{\sin(\psi_{ij}/T)}\right)\right]. \qquad (39)$$

Numerical results

Equation (32) is an expression for the bias error in estimating the frequency response when the cross-spectra between inputs are neglected. Note that in order to estimate the bias error, estimates of the other frequency responses are needed. Several example will be discussed to show the form of the bias error and the effect, of the assumption that the product $S(f)H_j(f)$ is relatively constant in any one band.

Example 1. Consider a six-input system where the inputs are mutually coherent band, limited white noise (constant spectral density) and the time delay between inputs is uniform and equal to 20 msec. The frequency responses are independent of frequency and have equal real and imaginary parts, as given by

$$H_i = Z_i(l+i),$$

where $Z_i = 1, 1, 2, 2, 3, 3$, for $i = 1, 2, \ldots, 6$, respectively. A band center-frequency of 208 Hz was chosen. Figure 7 shows the computed and actual bias error for $\hat{H}_1$ as a function of analysis bandwidth B_e, where the solid lines are the real and imaginary bias error calculated from equation (32) and the symbols are actual bias errors determined by estimating H_1 from equation (13), where cross-spectra between inputs have been neglected. The theoretical error

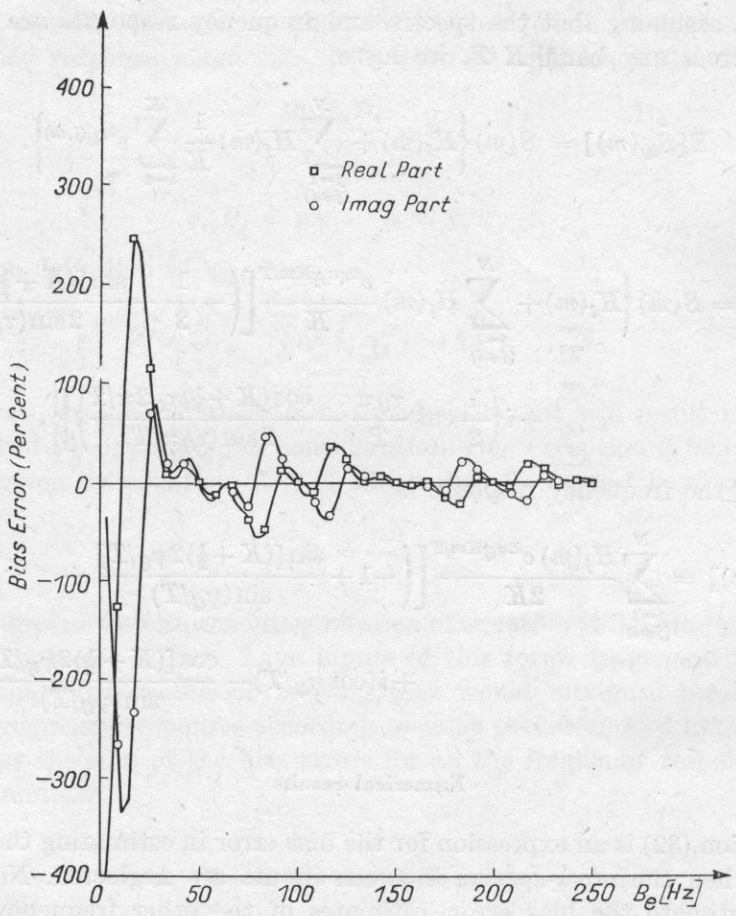

Fig. 7. Computed and theoretical bias error for Example 1

predicts exactly the actual error. The bias error is smaller for larger bandwidths due to the effect of frequency smoothing, which is really spectrum integration od $S_{iy'}$ (equation (26)). The cross-spectral terms of $S_{iy'}$ (equation (9)) are oscillatory in frequency, being both positive and negative, and tend to cancel when integrated, while the direct term, $H_1 S_{11}$, is positive across the entire band. As can be seen from Fig. 7, complete cancellation of the cross-spectral terms occurs at bandwidths that are multiples of 50 Hz. Since the delay between inputs is 20 msec, the fundamental frequency of the inputs is 8.333... Hz $(1/(6 \times 0.020))$ and the cross-terms cancel at every bandwidth that is a multiple of six times the fundamental frequency or every 50 Hz. This is analogous to the examples in Figs. 5 and 6.

Example 2. *Non-uniform delay between inputs.* In this example the time delay between inputs 1 and 2, 3 and 4, 5 and 6 is 15 msec and the time delay

between inputs 2 and 3, 3 and 4 and 6 and 1 is 25 msec, while the frequency responses and the input spectral densities are the same as in Example 1. Figure 8 shows the computed and actual bias error of $\hat{H}_1$ for this example at 208 Hz where it is again noted that equation (32) exactly predicts the actual bias error. In this case, however, a bandwidth of zero bias error for both real and imaginary parts of $\hat{H}_1$ does not occur until $B_e = 200$ Hz, although the error is quite small at 125 and 150 Hz.

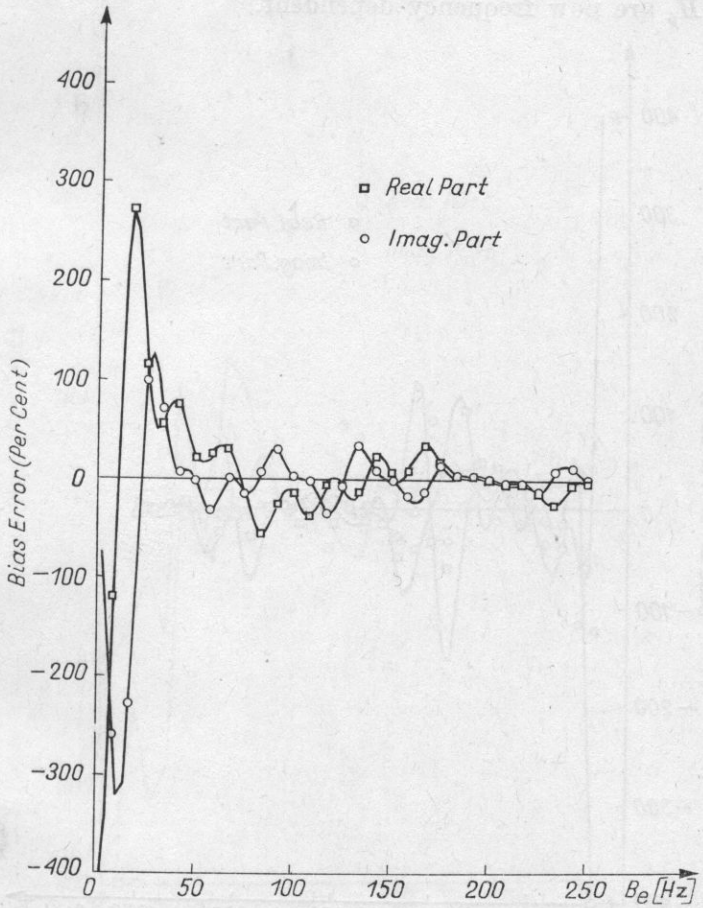

Fig. 8. Computed and theoretical bias error for Example 2

Example 3. *Frequency dependent response functions.* For this example H_1 is the same as in the previous examples, but H_1-H_6 are chosen to be second-order systems with the relation

$$H_i(f) = \frac{Z_i}{1+2\xi\left(\frac{f}{f_i}\right)i-\left(\frac{f}{f_i}\right)^2}, \qquad i = 2, 3, \ldots, 6,$$

where Z_i is as in the previous examples, the damping ratio $\xi = 0.1$, and the natural frequencies $f_i = 180$, 200, 220, 240 and 260 Hz for $i = 2, 3, \ldots, 6$. The time delay between inputs was as in Example 1. Figure 9 shows the computed and actual bias error for $\hat{H}_1$ in a band centered at 208 Hz. It can be seen from Fig. 9 that equation (32) has become inaccurate in predicting the bias error, particularly at certain frequencies. This is a result of the violation of the assumption that $H_i S_{ii}$ is relatively constant across the bandwidth, since the functions H_2-H_6 are now frequency dependent.

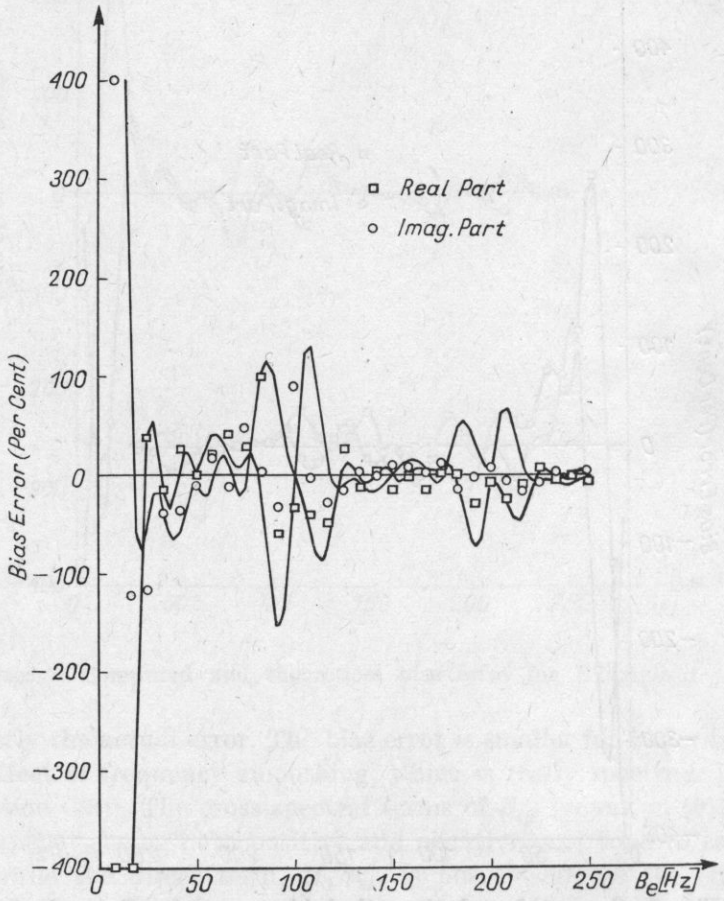

Fig. 9. Computed and theoretical bias error for Example 3

If the analysis band contains, or is near one or more of the natural frequencies, the bias error will not be accurately predicted by equation (32), particularly if the damping is low; the presence of natural modes in a band increases the frequency dependence of the frequency response.

To predict a more accurate bias error than equation (32) one would expand the estimates of the frequency responses in the Taylor series about the band

center-frequency, place the series in equation (28), and proceed as before, omitting the assumption that $H_i S_{ii}$ is constant. This would yield an expression similar to equation (32), but including terms that would be functions of the first and higher derivatives of the frequency responses. Thus, it would then be necessary to have estimates of not only the frequency responses, but also the derivatives of the frequency responses. The number of terms in the Taylor series needed accurately to predict the error would depend on the variation of the frequency responses within the bandwidth.

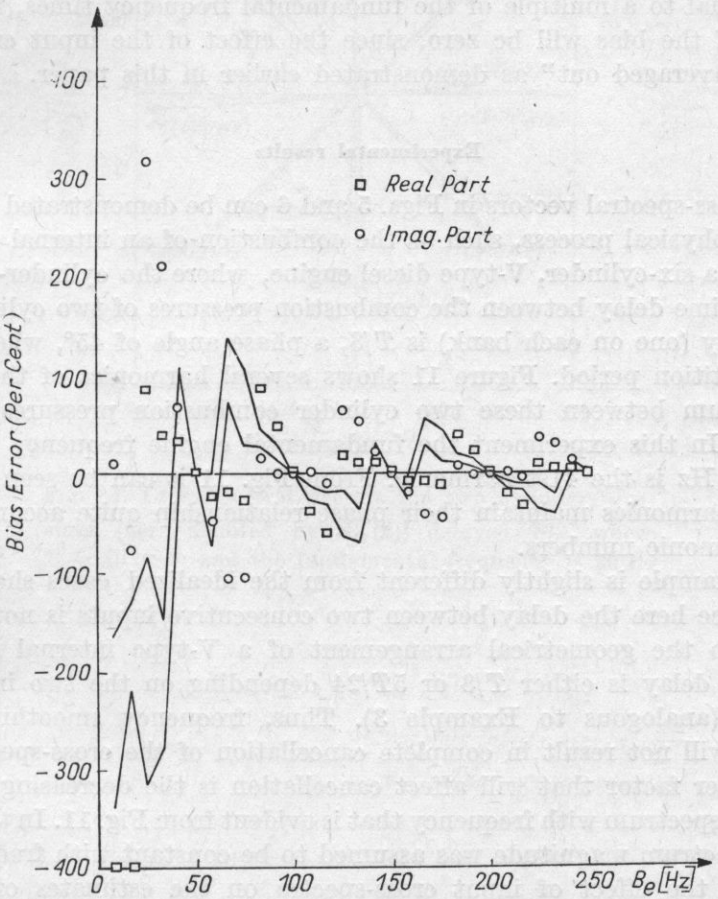

Fig. 10. Computed and theoretical bias error for Example 4

Example 4. *Deterministic inputs.* In this example the time delays and frequency responses are as in Example 1 while the inputs are delta functions in time (constant spectrum level). The only difference from the first example occurs in the analysis bandwidth; here bandwidth is restricted to a multiple of the fundamental frequency $1/T$, where $T = 120$ msec is the fundamental period of all inputs. Figure 10 is a plot of the computed bias error of $\hat{H}_1$ (equa-

tion (39)) and the actual error, showing that the error is accurately predicted only at the bandwidths of zero bias error. The failure of equation (39) to predict the bias is related to the difference in equations (26) and (36) where an integral has been replaced by a summation of a finite number of terms. The integrand S_{iy} is composed of a set of cross-terms which are highly frequency dependent (see equation (28)). Therefore, when the system inputs are deterministic and S_{iy} is estimated by smoothing in the frequency domain, severe bias can be introduced since the raw spectrum is not a continuous function. When the bandwidth is equal to a multiple of the fundamental frequency times, the number of inputs of the bias will be zero, since the effect of the input cross-spectra has been "averaged out" as demonstrated earlier in this paper.

Experimental results

The cross-spectral vectors in Figs. 5 and 6 can be demonstrated experimentally for a physical process, such as the combustion of an internal combustion engine. For a six-cylinder, V-type diesel engine, where the cylinder-bank angle is 90°, the time delay between the combustion pressures of two cylinders firing consecutively (one on each bank) is $T/8$, a phase angle of 45°, where T is the engine repetition period. Figure 11 shows several harmonics of the measured cross-spectrum between these two cylinder combustion pressures, beginning at 820 Hz. In this experiment the fundamental engine frequency was 20 Hz, so that 820 Hz is the 41st harmonic. From Fig. 11 it can be seen that cross-spectrum harmonics maintain their phase relationship quite accurately, even at high harmonic numbers.

This example is slightly different from the idealized cases shown in Fig. 5 and 6 since here the delay between two consecutive inputs is not a uniform T/N due to the geometrical arrangement of a V-type internal combustion engine; the delay is either $T/8$ or $5T/24$ depending on the two inputs being considered (analogous to Example 3). Thus, frequency smoothing over N harmonics will not result in complete cancellation of the cross-spectra in this case. Another factor that will affect cancellation is the decreasing magnitude of the cross-spectrum with frequency that is evident from Fig. 11. In the idealized case the spectrum magnitude was assumed to be constant with frequency.

To see the effect of input cross-spectra on the estimates of frequency response, the frequency response was computed between one of the cylinder pressure inputs and the engine noise (at 1 m form one side), with and without the cross-spectra. For the case where the input cross-spectra were included, equation (1) was solved for the frequency response matrix. Equation (7) was used to estimate the frequency response for the case where the input cross-spectra were neglected. Figure 12 shows one of the frequency responses computed for both cases. The bandwidth used in the analysis was 140 Hz corresponding to a frequency smoothing of seven harmonics in each band (20 Hz

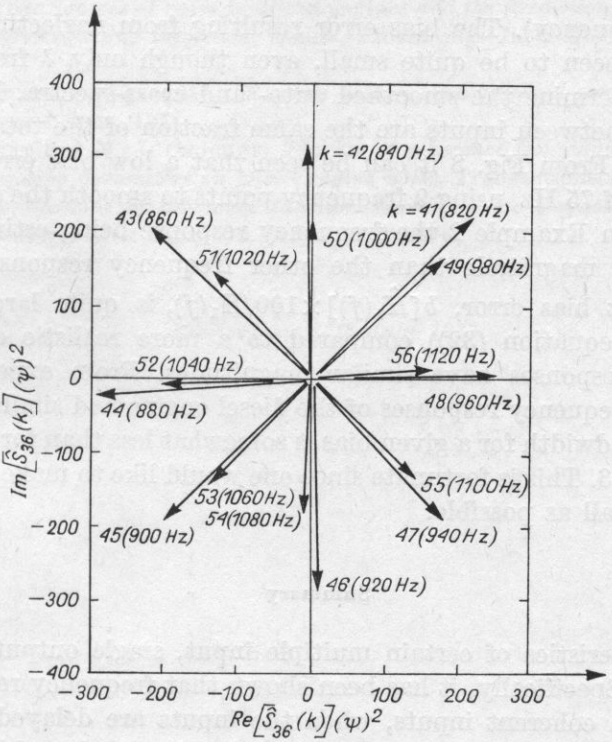

Fig. 11. Cross-spectral vectors for two cylinder pressures (here denoted by $\hat{S}_{36}(k)$) delayed $T/8$, where $T = 50$ msec and the fundamental frequency is 20 Hz

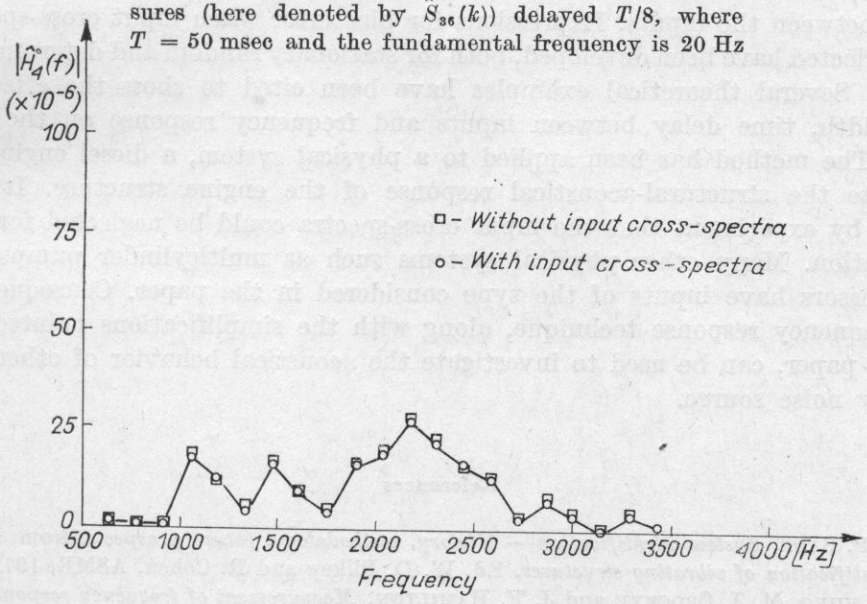

Fig. 12. Frequency response magnitude linear scale as a function of frequency, computed with and without considering input cross-spectra

fundamental frequency). The bias error resulting from neglecting input cross--spectra can be seen to be quite small, even though only 7 frequency points were used to determine the smoothed auto- and cross-spectra. In Example 2, the time delays between inputs are the same fraction of the total time T as in this experiment. From Fig. 8 it can be seen that a low bias error is predicted at a bandwidth of 75 Hz, using 9 frequency points to smooth the spectra instead of 7. However, in Example 2 the frequency response being estimated, H_1 was much smaller in magnitude than the other frequency responses (H_2-H_6) so that the percent bias error, $b[\hat{H}_1(f)] \times 100/H_1(f)$, is quite large for a given bandwidth (see equation (32)) compared to a more realistic example where the frequency responses have similar magnitudes. From experiment it was found that the frequency responses of the diesel engine had similar magnitudes; therefore the bandwidth for a given bias is somewhat less than for the theoretical case in Example 3. This is fortunate since one would like to make the bandwidth resolution as small as possible.

Summary

The characteristics of certain multiple input, single output systems have been discussed. Specifically, it has been shown that frequency responses can be determined from coherent inputs, when the inputs are delayed in time. It is shown that there exists an optimum analysis bandwidth for which the analysis is valid, and the bandwidth is related to the number of inputs and the time delay between the inputs. Expressions for bias error when input cross-spectra are neglected have been developed, both for stationary random and deterministic inputs. Several theoretical examples have been cited to show the effect of bandwidth, time delay between inputs and frequency response on the bias error. The method has been applied to a physical system, a diesel engine, to estimate the structural-acoustical response of the engine structure. It was shown by experiment that the input cross-spectra could be neglected for this application. Many other physical systems such as multicylinder pumps and compressors have inputs of the type considered in the paper. Consequently, the frequency response technique, along with the simplifications pointed out in this paper, can be used to investigate the acoustical behavior of other machinery noise source.

References

[1] A. P. Sage, *System identification – History, methodology, future prospects*, from *System identification of vibrating structures*, Ed. W. D. Pilkey and R. Cohen, ASME, 1972.

[2] J. Chung, M. J. Crocker and J. F. Hamilton, *Measurement of frequency response and the multiple coherence function of the noise generation system of a Diesel engine*, JASA, **58**, 3, 635 (1975).

[3] M. J. Crocker, *Sources of noise in Diesel engines and the prediction of noise from experimental measurements and theoretical models*, Proceedings Inter-Noise 75, August 27-29, 1975, 259.

[4] J.S. Bendat and A.G. Piersol, *Random data — Analysis and measurement procedures*, John Woley and Sons, 1971.

[5] A. F. Seybert and M. J. Crocker, *The use of coherence techniques to predict the effect of engine operating parameters on Diesel engine noise*, Transactions ASME, **97**, B, 4.

[6] — *Recent applications of coherence function techniques in diagnosis and prediction of noise*, Proceedings Inter-Noise 76, April 5-7, 1976.

Received on 27th July 1977

ARCHIVES OF ACOUSTICS
3, 3, 175-184 (1978)

PROPERTIES OF SOME ACOUSTO-OPTICAL MATERIALS

ZYGMUNT KLESZCZEWSKI

The Institute of Physics, Silesian Technical University, 44-100 Gliwice, ul. B. Krzywoustego 2

The paper discusses the requirements to be met by the acousto-optical materials. Utilizing the scattering of laser light by acoustic wave, the measurements of the propagation velocity and absorption coefficients of acoustic waves and the photoelastic constants for $Bi_{12}GeO_{20}$, $Bi_{12}SiO_{20}$, TiO_2 crystals and for SF-14 flint glass were made. On the basis of the above measurements acousto-optical parameters of the examined crystals have been calculated and subsequently discussed.

1. Introduction

A rapid development of laser techniques and the possibility to generate acoustic waves over a wide frequency range have made the light—sound interaction the subject of significant practical importance. The experience acquired in this field has enabled the development of devices operating on the principles of this interaction, e.g. modulators and optical deflectors.

One of the basic problems in designing and developing the acousto-optical devices is the choice of suitable acousto-optical materials.

In this paper the requirements to be met by acousto-optical materials and the possibility to define their parameters on the basis of their physical and chemical properties will be discussed. Subsequently the results of measurements of acoustic and acousto-optical properties of some crystals available on the market, which may be applicable in acousto-optics, will be presented.

2. Parameters of acousto-optical materials

The materials used in acousto-optics should feature a high efficiency of light—sound interaction. This efficiency is described by the ratio of the intensity light diffracted by the acoustic wave to the intensity of incident light.

For the Bragg diffraction the ratio takes [5] the form

$$\eta = \frac{I}{I_0} = \frac{\pi^2}{2} \frac{n^6 p^2}{\varrho v^3} \frac{P_a L}{H \lambda_0^2 \cos^2 \theta}, \tag{1}$$

where I_0 is the intensity of incident light, I — the intensity of diffracted light, n — the optical refraction index, p — the photoelastic constant, ϱ — the density of medium, θ — the angle of difraction of laser beam, v — the velocity of acoustic wave propagation, λ_0 — the wavelength of light in vacuum, P_a — the power of acoustic beam, L and H are the length of light path through acoustic beam and the height of acoustic beam, respectively.

The expression $n^6 p^2/\varrho v^3$, appearing in (1), contains only material constants of the crystal. This expression will be denoted by M_2, as it is generally accepted in the literature [8].

Apart from high efficiency of light—sound interaction the acousto-optical materials should operate at a given angle of diffraction θ over as wide frequency range of acoustic waves as possible. This is made feasible by the use of an acoustic and laser beam with some divergence. It follows from theoretical calculations [2] that the best conditions of such an operation exist when divergencies of these beams are equal. It can be demonstrated that in this case the product of the efficiency of interaction η, the fundamental frequency f_0 and the band width Δf assumes the form

$$\eta f_0 \Delta f = \left(\frac{n^7 p^2}{\varrho v}\right) \frac{\pi^2 P_a}{\lambda_0^3 H \cos\theta}, \tag{2}$$

where Δf is the frequency range of the acoustic wave in which the intensity of diffracted light is reduced by 3 dB, f_0 — the fundamental frequency at which the intensity of diffracted light attains its maximum.

The expression $n^7 p^2/\varrho v$ is denoted by M_1 [3].

Frequently the third quantity

$$\eta f_0 = \pi^2 \left(\frac{n^7 p^2}{\varrho v^2}\right) \frac{P_a}{\lambda_0^3 \cos\theta} \tag{3}$$

is introduced which, unlike expressions (1) and (2), does not vary with the size of the acoustic beam. Material constant $n^7 p^2/\varrho v^2$ is denoted by M_3 [1].

It can be concluded that acousto-optical crystals should exhibit high values of the optical refraction index and photoelastic constants as well as a possibly low density and velocity of acoustic wave. It is also essential that the absorption of acoustic wave should be low. Furthermore, the crystals should meet several other requirements, the most important being:

1. high optical quality,
2. high chemical resistance and mechanical strength,
3. small temperature coefficients of physical constants.

3. Physico-chemical properties and acoustical parameters of crystals

Before the decision on growing a particular crystal can be made it is often desirable to gain some insight as regards the applicability of the crystals in acousto-optics, i.e. to be able to estimate the values of the velocity of acoustic

wave, photoelastic constants and optical refraction index. In the sequel a brief description will be given of the relationship between the physico-chemical properties of crystals and the velocity of acoustic wave and photoelastic constants.

A. *Velocity of sound.* For estimating the velocity of sound [7] the empirical formula

$$\log \frac{v}{\varrho} = -b\bar{M} + d \tag{4}$$

is very often used, where b and d are constants for a given type of crystals, $\bar{M}$ is the mean atomic weight, ϱ — the density of crystal, v — the velocity of acoustic wave.

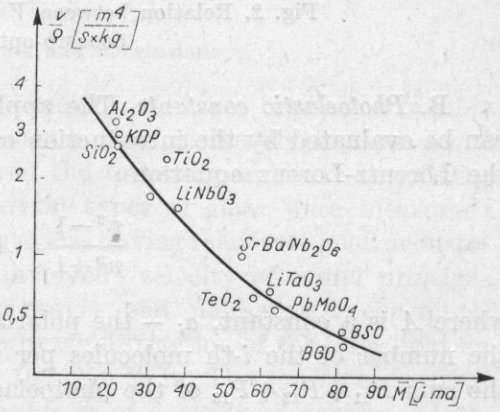

Fig. 1. Relation between V/ϱ and $\bar{M}$ for some acousto-optical crystals

Fig. 1 presents the dependence v/S on $\bar{M}$ for some substances. From this dependence it can be concluded that small velocities of sound can be anticipated for crystals with a high $\bar{M}$. The calculation of the velocity of sound — according to formula (4) — agrees within 25 % with the experimental values. In estimating the velocity of sound we also use [7, 9] formula

$$v = \sqrt{C\frac{T_t}{\bar{M}}}, \tag{5}$$

where T_t is the melting point, C — the constant for a given type of crystals, $\bar{M}$ — the mean atomic weight.

It seems that (5) is especially useful because it permits us to estimate the velocity of acoustic wave from conditions in which acousto-optical crystals are grown. Fig. 2 shows the dependence of v on T_t/M for some crystals. Similarly to the previous estimation, small velocities of acoustic wave can be anticipated for the crystals with high mean atomic weight and a low melting temperature at the same time.

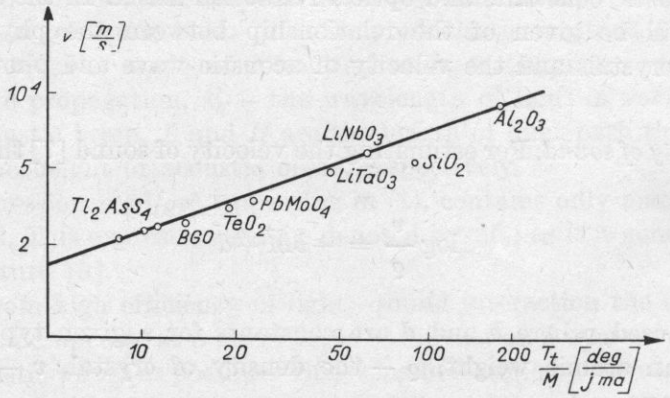

Fig. 2. Relation between V and the ratio T_t/M for some acousto-optical crystals

B. *Photoelastic constants.* The applicability of materials in acousto-optics can be evaluated by the introduction of the mean photoelastic constant. From the Lorentz-Lorenz equation

$$\frac{n^2-1}{n^2+1} = A \sum_i N_i a_i, \tag{6}$$

where A is a constant, a_i – the polarizability of the i-th molecule, and N_i – the number of the i-th molecules per unit volume, it is possible to calculate the sum $P_{11}+P_{12}+P_{13}$ of the photoelastic constants or the mean photoelastic constant

$$P_m = \frac{P_{11}+P_{12}+P_{13}}{3} = -\frac{(n^2-1)(n^2+2)}{3n^4}(1-\Lambda_0), \tag{7}$$

where

$$\Lambda_0 = \frac{\varrho}{a}\frac{da}{d\varrho}.$$

For all materials of interest for acousto-optics $n > 1{,}5$ and thus, to a good approximation,

$$P_m = 0{,}35(1-\Lambda_0). \tag{8}$$

It follows that the value of photoelastic constants does not actually depend on the optical refraction index but is determined by the change in polarizability when the density of crystal is changed. These changes depend essentially on the type of crystal bonds. In crystals with an ionic bonding the polarizability increases with the increase of the atomic weight, since the outer electrons are less strongly bound to nuclei, the polarizability of the positive ions being smaller than that of the negative ones. If an ionic crystal is subjected to compression,

the polarizability of the positive ion increases and that of the negative ion decreases. Hence $da/d\varrho < 0$, and $A_0 > 0$.

Experimental data indicate that $A_0 \cong 0.5$ for the ionic crystals. If the contribution of the covalent bonding in the crystal increases, then values of the photoelastic constants are dependent on two competing processes: the change of polarizability under pressure and the change of packing density. On the other hand, in crystals with a purely covalent bonding, there can be observed an intense decrease of the molecular polarizability due to the increased packing density. Consequently, crystals with a purely covalent bonding have a large A_0 and, therefore, exhibit weak acousto-optical properties.

Concluding, good acousto-optical properties should be expected for crystals with a very high mean atomic mass, low melting temperature and ionic or ionic-covalent bondings.

4. Results of experiments and conclusions

Measurement of acousto-optical parameters of some crystals available in the market, which can be used in acousto-optics, primarily in laser hight modulators, were made. The tests involved the following crystals: $Bi_{12}\ GeO_{20}$ (BGO), $Bi_{12}\ SiO_{20}$ (BSO), TiO_2. Also certain types of glass were measured; particular attention was devoted to the flint-glass having relatively good acousto-optical parameters. The measurements involved: velocity of sound propagation, absorption coefficients of acoustic waves and photoelastic constants. The measurements were made using the Bragg diffraction of the laser light on an acoustic wave over the frequency range 100 - 700 MHz. The source generating the longitudinal acoustic waves were transducers of quartz and lithium iodate, glued directly to the examined crystal or to the fused quartz, the latter being used as a reference substance.

The measuring system used is described in detail in [4].

The velocity of acoustic wave propagation was calculated from the measurement of Bragg angle according to the formula

$$v = \frac{\lambda_0 \nu}{2n \sin\theta}. \tag{9}$$

On the basis of the velocity of propagation, the elastic constants C_{ij} of the examined crystals were determined.

The elastic constants were determined by the measurement of the intensity of diffracted light in the examined crystal and in the reference substance (fused quartz) glued to the crystal.

It can be seen from relation (1) that the intensity of diffracted light is proportional to P^2 and it is easy to show that

$$P_x = P_0 \left(\frac{n_0}{n_x}\right)^3 \frac{\varrho_x v_x^3}{\varrho_0 v_0^3} \left(\frac{I_{1x} I_{2x}}{I_{10} I_{20}}\right)^{1/4} \frac{1 - R_0}{1 - R_x}, \tag{10}$$

where I_{1x}, I_{2x}, I_{10}, I_{20} are the intensities of light diffracted on the incident wave and refracted in the tested crystal and in the reference material. The subscript x refers to the tested substance, the subscript 0 — to the reference substance,

$$R_0 = \left(\frac{n_0 - 1}{n_0 + 1}\right)^2, \qquad R_x = \left(\frac{n_x - 1}{n_x + 1}\right)^2.$$

For the fused quartz it was assumed that $P_{11} = 0.12$, $P_{12} = 0.27$. Table 1 summarizes the results of measurements. The accuracy of the velocity measurement is 0.2 % and that of photoelastic constants — 10 %.

Table 1. Velocity of the propagation of acoustic waves, elastic and photoelastic constants of the examined substances

Substance, crystallographic structure	n	ϱ 10^3 [kg/m^3]	Direction of the propagation of acoustic wave	v [m/s]	Elastic constants	Photoelastic constants
SF-14 Glass	1.76	4.54	—	3580	$C_{11} = 0.58$	$P_{11} = 0.14$ $P_{12} = 0.135$
BGO						
(cubic 23)	2.55	9.22	[100]	3740	$C_{11} = 1.29$	$P_{11} = 0.12$
			[110]	3398	$C_{12} = 0.30$	
			[111]	3276	$C_{44} = 0.26$	$P_{44} = 0.04$
BSO						
(cubic 23)	2.55	9.21	[100]	3727	$C_{11} = 1.28$	$P_{11} = 0.13$
			[110]	3350	$C_{12} = 0.27$	
			[111]	3217	$C_{44} = 0.25$	$P_{44} = 0.04$
TiO_2						
(tetragonal 4/mmm)	2.58	4.23	[110]	7930	$C_{11} = 2.72$	$P_{11} = 0.01$
			[010]	7930	$C_{12} = 1.76$	$P_{13} = 0.16$
			[110]	9827	$C_{66} = 1.95$	$P_{31} = 0.10$

Also the measurements of the absorption coefficient of acoustic waves for the examined crystals were made, since it is known that this coefficient is essential in considering the application of a given material in acousto-opticla devices.

The measurements of the absorption coefficient were made using the method of stationary waves, and also by the measurement of intensity of diffracted light on the incident wave at different distances from the transducer.

In the former case, when the frequency of a continuous acoustic wave changes insignificantly, the intensity of diffracted light varies periodically between the maximum and the minimum values. The absorption coefficient was determined from the relation

$$a\left[\frac{\text{dB}}{\text{cm}}\right] = \frac{8.686}{L} \operatorname{ar}\tanh\left(\frac{I_{\min}}{I_{\max}}\right)^{1/2}, \tag{11}$$

where L is the length of crystal, $I_{\min}$ and $I_{\max}$ – the intensities of light at the minimum and maximum, respectively.

In the latter case the absorption coefficient was calculated according to the formula

$$a\left[\frac{\mathrm{dB}}{\mathrm{cm}}\right] = \frac{8.686}{2(x_2 - x_1)} \ln \frac{I(x_1)}{I(x_2)}, \tag{12}$$

where $I(x_1)$ and $I(x_2)$ are the intensities of diffracted light at distances x_1 and x_2 from the transducer, respectively.

The results of measurements obtained for the absorption coefficient are shown in Figs. 3-5. The accuracy of measurement of the absorption coefficient is about 10%.

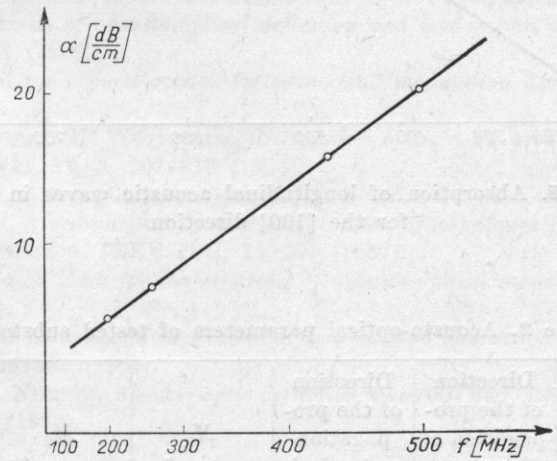

Fig. 3. Absorption of longitudinal acoustic waves in SF-14 glass

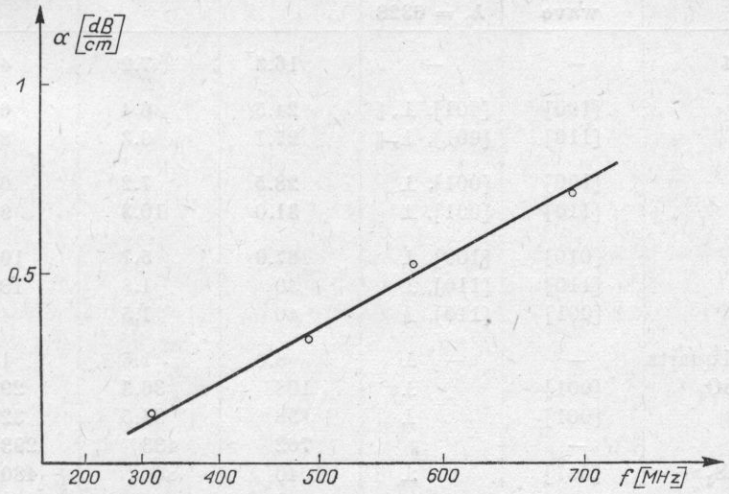

Fig. 4. Absorption of longitudinal acoustic waves in TiO_2 for the [110] direction

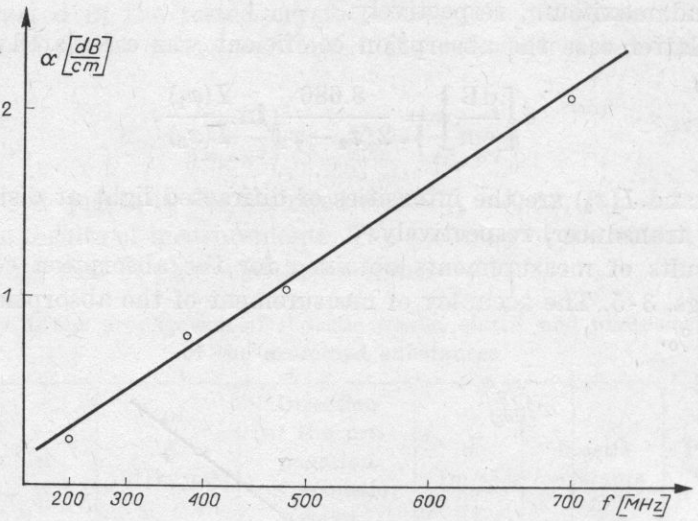

Fig. 5. Absorption of longitudinal acoustic waves in BGO for the [100] direction

Table 2. Acousto-optical parameters of tested substances

Substance	Direction of the propagation of longitudinal acoustic wave	Direction of the propagation and polarization of light $\lambda_0 = 6328$	M_1 $10^{-8}\left[\frac{m^2\,s}{kg}\right]$	M_2 $10^{-15}\left[\frac{s^3}{kg}\right]$	M_3 $10^{-11}\left[\frac{ms^2}{kg}\right]$
SF-14	—	—	16.3	7.2	4.5
BGO	[100]	[001], ⊥, ∥	24.5	6.4	6.6
	[110]	[001], ⊥, ∥	27.1	9.3	8.0
BSO	[100]	[001], ⊥	28.5	7.2	6.3
	[110]	[001], ⊥	31.0	10.3	9.2
TiO_2	[010]	[100], ⊥	67.9	5.7	10.0
	[110]	[110], ⊥	30	1.8	18.4
	[001]	[110], ⊥	40	1.5	4.0
Fused quartz	—	— ⊥	8.0	1.6	1.3
$PbMoO_4$	[001]	⊥	108	36.3	29.8
TeO_2	[001]	⊥	138	34.5	32.8
As_2S_3	—	∥	762	433	293
Tl_3AsS_4	[001]	⊥	1040	800	480

∥ or ⊥ — polarization of light parallel or normal to diffraction plane

On the basis of these measurements the values of the parameters M_1, M_2 and M_3 (Table 2) for the examined crystals were calculated. For comparison the values of these parameters for the fused quartz, which is frequently used in acousto-optical measurements, are also enclosed. The data for these substances were taken from paper [9]. It results from the comparison that the examined crystals, especially BGO and BSO, exhibit quite good acousto-optical properties, but are inferior to such crystals as $PbMoO_4$ or TeO_2.

References

[1] R. W. Dixon, *Photoelastic properties of selected materials and their revelance for applications to acoustic light modulators and scanners*, J. Appl. Phys., **38**, 13, 5149-5153 (1967).

[2] E. I. Gordon, *Review of acousto-optical deflection and modulation devices*, Proc. IEEE, **54**, 1P, 1391-1401 (1966).

[3] — *Figure of merit for acousto-optical deflection and modulation devices*, IEEE-JQE, **2**, 104-105 (1966).

[4] Z. Kleszczewski and M. Wojewoda, *Diffraction of light on acoustic waves in solids*, Archiwum Akustyki, **11**, 2, 207-216 (1976).

[5] *Physical Acoustics*, v. 7, Academic Press, ed. W. P. Mason, New York (1968).

[6] P. H. Mc Mahon, *A comparison of Brillouin scattering techniques for measuring microwave acoustic attenuation*, IEEE-TSU, **14**, 103 (1967).

[7] P. D. Pinnow, *Guide lines for the selection of acousto-optical materials*, IEEE-JQE, **6**, 4, 233-238 (1970).

[8] T. M. Smith and A. Korpel, *Measurement of light—sound interaction efficiencies in solids*, IEEE-JQE, **1**, 283-284 (1965).

[9] N. Uchida and N. Niizeki, *Acousto-optic deflection materials and techniques*, Proc. IEEE, **61**, 8, 1073-1092 (1973).

Received on 7th November 1977

ARCHIVES OF ACOUSTICS
3, 3, 185-196 (1978)

THE ZERO-CROSSING ANALYSIS OF A SPEECH SIGNAL IN THE SHORT-TERM METHOD OF AUTOMATIC SPEAKER IDENTIFICATION

CZESŁAW BASZTURA, JERZY JURKIEWICZ

Institute of Telecommunication and Acoustics, Technical University,
50-317 Wrocław, ul. B. Prusa 53/55

The aim of this paper is to investigate the possibility of using the zero-crossing analysis of a speech signal in a short-term method of speaker identification. Four sets of parameters obtained with the aid of the zero-crossing analysis are presented which can find application in automatic speaker identification. An experiment of speaker identification for 20 male speakers has been performed. The obtained results have confirmed the applicability of the method of zero-crossing analysis for tracking individual features of voices.

1. Introduction

Thecom plex ityfo the speech process both as regards its mental and articulatory aspect is manifested by the occurrence in a speech signal of a multitude of extralinguistic information, including also that about individual features of speaker's voice. Practice has shown that individual features contained in a speech signal enable the recognition of a speaker on the basis of his statements.

The main stimulus for investigations on the automatic speaker identification is the development of computer techniques and the availability of computers for the processing of the speech signal. Automatic speaker identification can be accomplished by using two identification models which differ primarily by the kind and duration of statement text.

The method based on the long-term analysis features some degree of independence on the text and a relatively long duration of statement. The method of the short-term analysis is based on the individual parameters of the voice obtained from fixed text in a time ranging from a fraction of a second for single phonems, up to several seconds for sentences. The short-term analysis method necessitates the use of time normalization of the signals to be analyzed or of vectors representing these signals in the adopted parameter space.

The speaker identification method should give an adequate and invariant description of the voices of speakers. The sets of parameters for the automatic speaker identification should be [1]:

1° effective in representation of individual features of speakers,
2° easy to measure,
3° stable over the required period of time,
4° little sensitive to ambient conditions changes,
5° hard to imitate.

So far no such set of parameters, which would satisfactorily meet all these requirements, has been found. In view of a complex structure of a speech signal and the lack of explicit premises the choice of the parameters discriminating the voices is dictated mostly by heuristic reasons based on the previous experiments, the acquired knowledge, and even intuition [1, 3, 6].

After such a choice has been made, it is necessary to substantiate it theoretically and experimentally in order to verify the assumed hypothesis of the practicability of the set of parameters used for the automatic speaker identification.

The results of investigations obtained by many authors have convincingly confirmed unquestionable advantages of the zero-crossing analysis of a speech signal, e.g. for the speaker identification and speech analysis [2, 4, 7].

The aim of this paper is to investigate the possibility of using the zero-crossing analysis of a speech signal for automatic speaker identification by the short-term method.

2. Methods of investigations

2.1. *Choice of the statement text.* For the methods based on the short-term analysis one chooses texts which are easy to pronounce, widely used and contain phonetic elements which provide as much as possible information on the individual features of speaker's voice.

The investigations carried out by many authors indicate that vowels as well as lateral, liquid and nasal consonants contribute most to the differentiation of individual features. This results from the fact that the phonation of vowels depends on the shape and size of the vocal tract of a speaker and the properties of the source of his laryngeal tone. The spectra of nasal consonants, however, are closely related to the nasal cavity and to its interaction with the mouth cavity. The position of the tongue and teeth greatly affects the articulation of the lateral consonants. In keeping with this consideration the word ALO has been chosen as a text for a statement.

An additional motivation for the choice of this word is its wide use in colloquial speech (as voiced part of the word HALO), especially when starting a phone conversation.

2.2. *The sets of parameters used for the description of individual features of speakers.* The creation of a suitable parameter space is regarded to be one of the most difficult stages in the process of the automatic speaker identification. It should be stressed that the determination of the values of parameters such as the fundamental frequency F_0 or the frequency of formants using the zero-crossing analysis (ZCA) is not accurate enough to justify the use of these parameters for speaker identification. For this reason it seems advisable to define, with the aid of the ZCA method, the other sets of parameters which satisfy, to some extent, the requirements listed in the introduction.

The description of individual features of voice presented in this paper has been based on the distribution of time intervals and parameters based on the time dependence of the density of zero-crossings of a speech signal.

(a) The function of zero-crossings of a signal.

For the time-dependent signal $U = U(t)$ the function $P(U, t)$ of a zero-crossing has been defined,

$$P(U,t) = \begin{cases} 1 & \text{if there exists } U(t) \text{ satisfying conditions (i)-(iii),} \\ 0 & \text{if there is no } U(t) \text{ satisfying conditions (i)-(iii),} \end{cases} \tag{1}$$

where

$$U(t)\,U(t-\tau) < 0, \tag{i}$$

$$|U(t)| \geqslant a \quad \text{and} \quad |U(t-\tau)| \geqslant a, \tag{ii}$$

$$|U(x)| < a \quad \text{for} \quad t-\tau < x < t, \tag{iii}$$

and a is a threshold level ($a \neq 0$) which prevents counting additional zero-crossings caused by disturbances [4].

The values t_i for which $P(U, t_i) = 1$ are the moments of the zero-crossing of the signal $U(t)$.

(b) Distributions of time intervals.

Using the function $P(U,t)$ makes it possible to present the time dependence of the signal $U(t)$ in a simpler form by means of segments of lengths t_j which are equal to the intervals between successive zero-crossings of a speech signal. For a given signal representing a selected text of a statement one can choose the limiting values t_d and t_g as extreme values of the time intervals between zero-crossings. If in the interval (t_d, t_g) we distribute $K-1$ threshold values, then we obtain K time channels. The values $y(t_{k-1}, t_k)$ represent the number of intervals t_j contained in the interval (t_{k-1}, t_k).

If the time dependent signal $U_{m,i}(t)$ of a duration $T_{m,i}$ constitutes a pattern of the m-th speaker and of the i-th repetition of the speaker's voice, then this pattern can be represented in the form of a K-dimensional vector

$$\boldsymbol{y}_{m,i} = \{y_{m,i,1}, y_{m,i,2}, \ldots, y_{m,i,k}, \ldots, y_{m,i,K}\}. \tag{2}$$

An example of the distribution of time intervals is shown in Fig. 1.

(c) Time dependence of the density of zero-crossings.

The results presented in paper [7] suggest that it is possible to use the time dependence of the density function of zero-crossings for voice discrimination. The measurement of the density $\varrho(kt_N) = \varrho[U(kt_N)]$ from a speech signal in discrete form U_n is made according to the relation

$$\varrho[U(kt_N)] = \frac{1}{t_N} \sum_{n=1}^{N} P\left(U_n, (k-1)t_N + \frac{n}{f_{\mathrm{pr}}}\right), \tag{3}$$

where k is the index of the signal segment of duration t_N, N – the number of signal samples in a given segment, f_{pr} – the sampling frequency, and $t_N = N/f_{\mathrm{pr}}$.

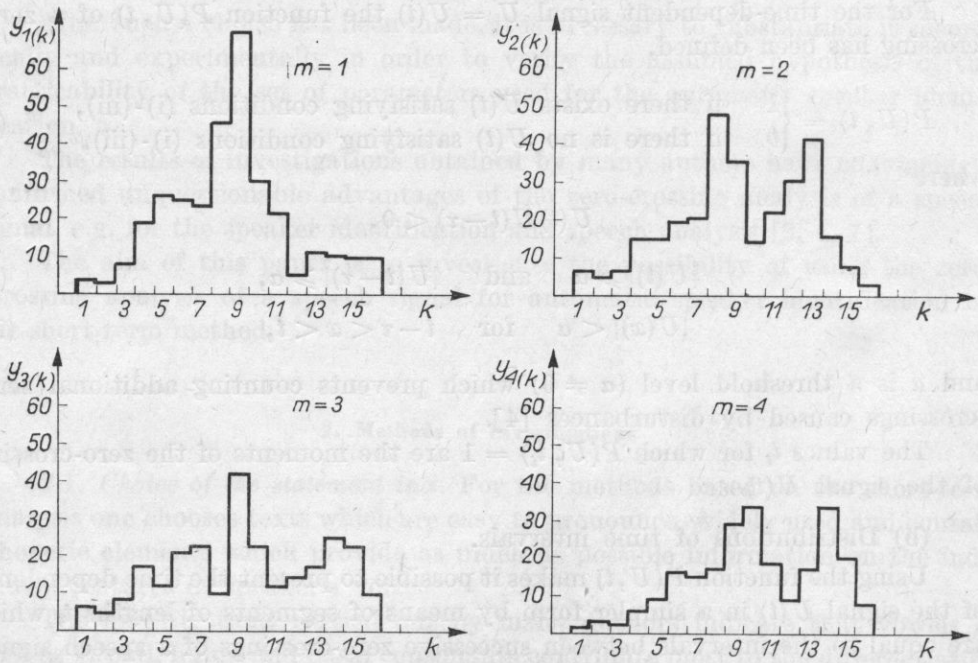

Fig. 1. The averaged distributions of time intervals for 4 speakers (averaging from 5 repetitions of statements)

The function $\varrho(kt_N)$ for the m-th speaker and the i-th repetition can be presented in the form of the vector

$$\boldsymbol{\rho}_{m,i} = \{\varrho_{m,i}(1), \varrho_{m,i}(2), \ldots, \varrho_{m,i}(K_{m,i})\}. \tag{4}$$

The dimension $K_{m,i}$ of the vector depends on the speaker, as also on the given repetition of the statement (especially as regards its rate) and this necessitates the use of time normalization [5].

(d) Parameters defined on the basis of the total time during which the points remain in given sectors of the phase plane $\{\varrho[U(t)], \varrho'[U(t)]\}$.

The time dependence of the zero-crossing density changes can be represented by the zero-crossing derivative. A speech signal can be described by a set of points with coordinates

$$\left\{\varrho[U(kt_N)], \frac{\Delta\varrho[U(kt_N)]}{t_N}\right\}$$

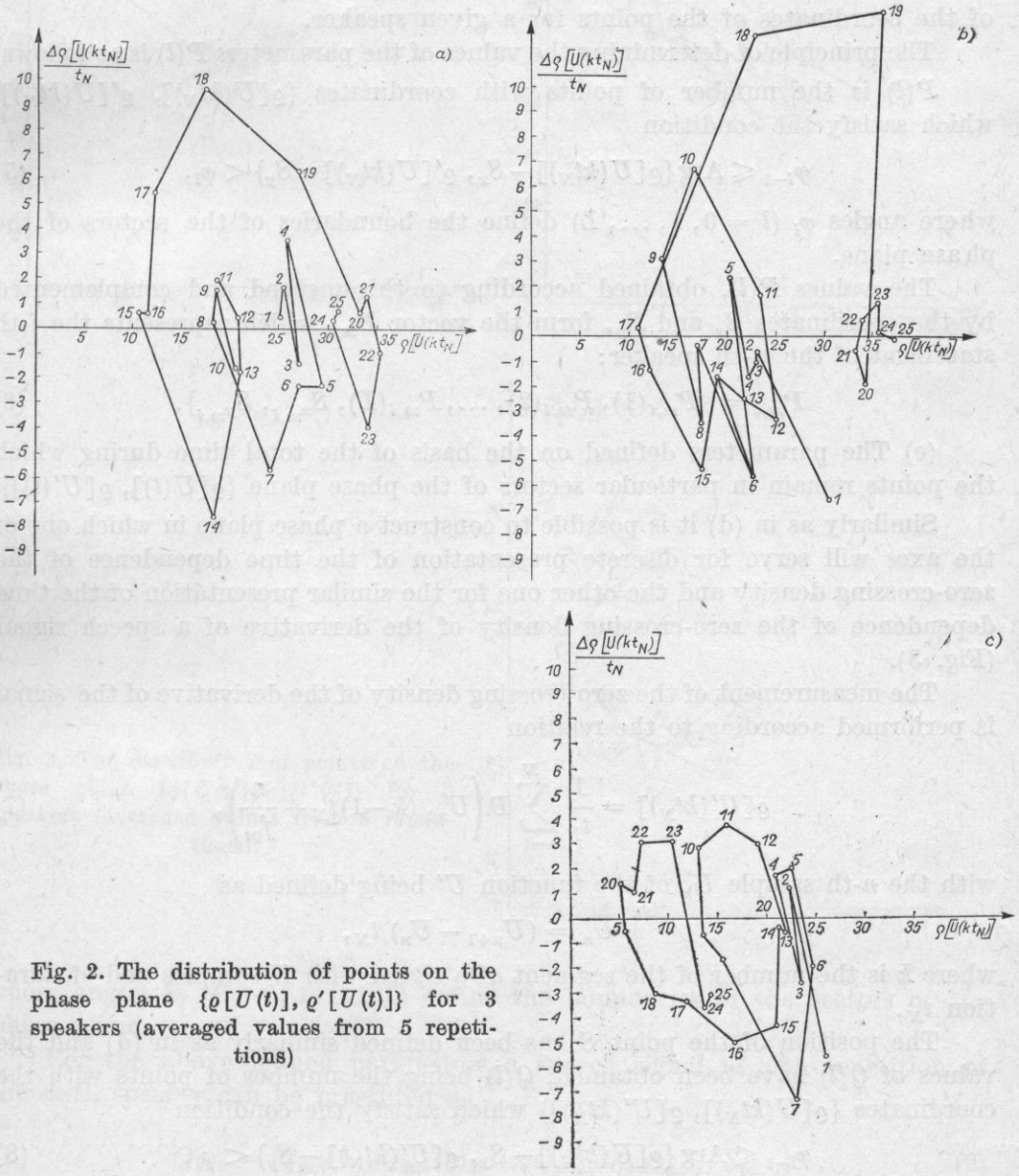

Fig. 2. The distribution of points on the phase plane $\{\varrho[U(t)], \varrho'[U(t)]\}$ for 3 speakers (averaged values from 5 repetitions)

belonging to the phase plane being a discrete representation of the plane $\{\varrho[U(t)], \varrho'[U(t)]\}$.

A given signal can also be characterized by the numbers $P(l)$ corresponding to the total time during which the points with indices $1, 2, \ldots, K_{m,i}$ remain in definite sectors of the phase plane (Fig. 2). By selecting a point S with coordinates S_x and S_y as a centre of the set of these points and assuming it as a central point of partition, it is possible to divide the phase plane into L sectors.

It is convenient to define the coordinates S_x and S_y as arithmetical means of the coordinates of the points for a given speaker.

The principle of determining the values of the parameters $P(l)$ is as follows:

$P(l)$ is the number of points with coordinates $\{\varrho[U(kt_N)], \varrho'[U(kt_N)]\}$ which satisfy the condition

$$\varphi_{l-1} \leqslant \operatorname{Arg}\{\varrho[U(kt_N)] - S_x, \varrho'[U(kt_N)] - S_y\} < \varphi_l, \tag{5}$$

where angles φ_l $(l = 0, 1, \ldots, L)$ define the boundaries of the sectors of the phase plane.

The values $P(l)$, obtained according to this method and complemented by the coordinates S_x and S_y, form the vector $\boldsymbol{P}_{m,i}$ which represents the i-th statement of the m-th speaker:

$$\boldsymbol{P}_{m,i} = \{P_{m,i}(1), P_{m,i}(2), \ldots, P_{m,i}(L), S_{x_{m,i}}, S_{y_{m,i}}\}. \tag{6}$$

(e) The parameters defined on the basis of the total time during which the points remain in particular sectors of the phase plane $\{\varrho[U(t)], \varrho[U'(t)]\}$.

Similarly as in (d) it is possible to construct a phase plane in which one of the axes will serve for discrete presentation of the time dependence of the zero-crossing density and the other one for the similar presentation of the time dependence of the zero-crossing density of the derivative of a speech signal (Fig. 3).

The measurement of the zero-crossing density of the derivative of the signal is performed according to the relation

$$\varrho[U'(kt_N)] = \frac{1}{t_N} \sum_{n=1}^{N} P\left(U'_n, (k-1)t_N + \frac{n}{f_{\mathrm{pr}}}\right), \tag{7}$$

with the n-th sample U'_n of the function U' being defined as

$$U'_n = (U_{n+1} - U_n)/t_N,$$

where k is the number of the segment of a signal with N samples and of duration t_N.

The position of the point S has been defined similarly as in (d) and the values of $Q(l)$ have been obtained, $Q(l)$ being the number of points with the coordinates $\{\varrho[U(kt_N)], \varrho[U'(kt_N)]\}$ which satisfy the condition

$$\varphi_{l-1} \leqslant \operatorname{Arg}\{\varrho[U(kt_N)] - S_x, \varrho[U'(kt_N)] - S_y\} < \varphi_l, \tag{8}$$

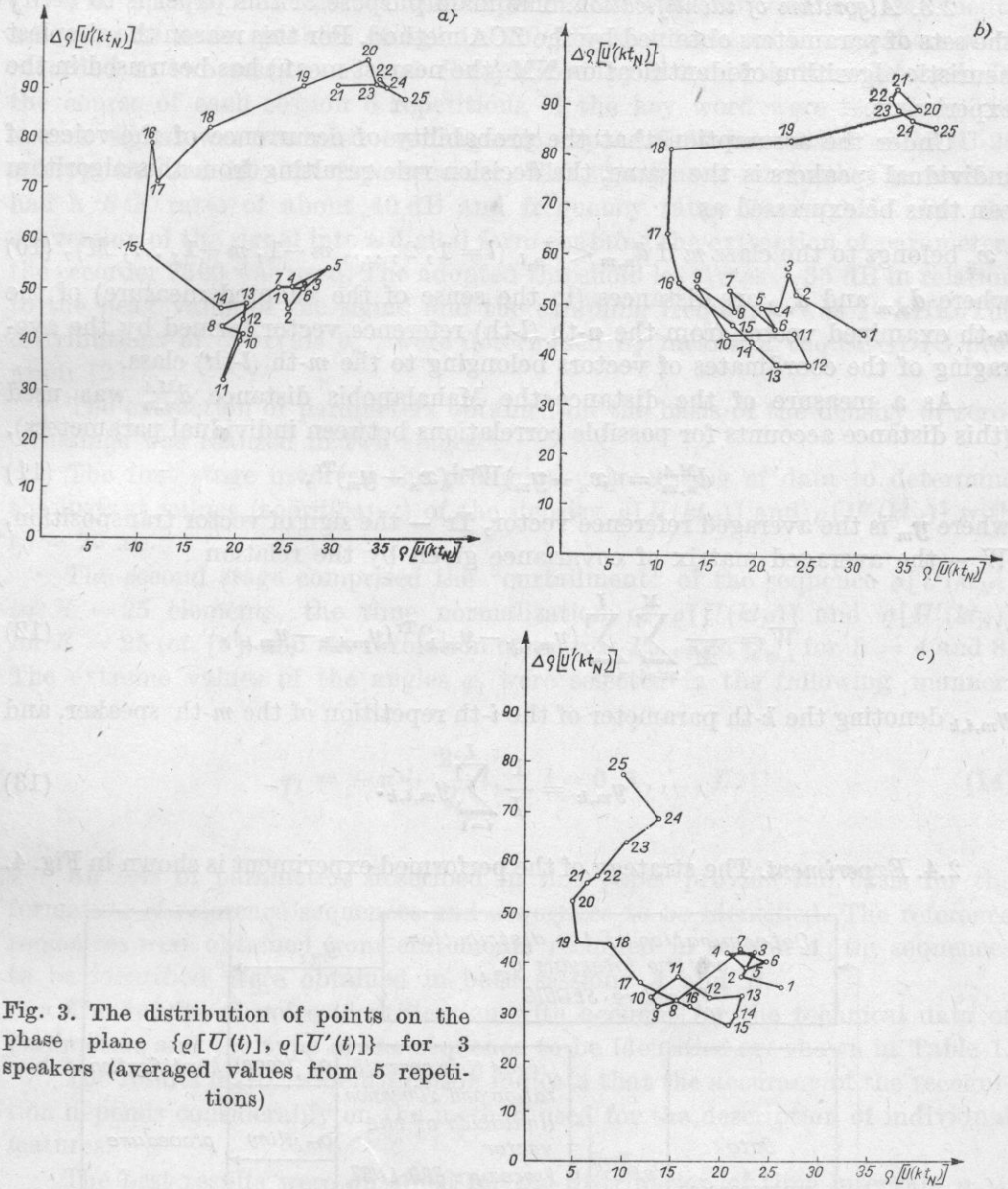

Fig. 3. The distribution of points on the phase plane $\{\varrho[U(t)], \varrho[U'(t)]\}$ for 3 speakers (averaged values from 5 repetitions)

where angles φ_l $(l = 0, 1, \ldots, L)$ define the boundaries of the sectors of the phase plane.

For the above-defined parameters a speech signal of i-th repetition of the m-th speaker can be presented as

$$\boldsymbol{Q}_{m,i} = \{Q_{m,i}(1), Q_{m,i}(2), \ldots, Q_{m,i}(L), S_{x_{m,i}}, S_{y_{m,i}}\}. \tag{9}$$

2.3. *Algorithm of identification.* The main purpose of this paper is to verify the sets of parameters obtained by the ZCA method. For this reason the simplest heuristic algorithm of identification NM (the nearest mean) has been used in the experiment.

Under the assumption that the probability of occurrence of the voices of individual speakers is the same, the decision rule resulting from this algorithm can thus be expressed as

$$\boldsymbol{x}_n \text{ belongs to the class } m \text{ if } d_{n,m} < d_{n,l} \quad (l = 1, 2, \ldots, m-1, m+1, \ldots, M), \tag{10}$$

where $d_{n,m}$ and $d_{n,l}$ are distances (in the sense of the adopted measure) of the n-th examined vector from the n-th (l-th) reference vector formed by the averaging of the coordinates of vectors belonging to the m-th (l-th) class.

As a measure of the distance the Mahalanobis distance $d_{n,m}^{MA}$ was used (this distance accounts for possible correlations between individual parameters),

$$d_{n,m}^{MA} = (\boldsymbol{x}_n - \boldsymbol{y}_m) W^{-1} (\boldsymbol{x}_n - \boldsymbol{y}_m)^{\mathrm{Tr}}, \tag{11}$$

where $\boldsymbol{y}_m$ is the averaged reference vector, Tr — the sign of vector transposition, W — the averaged matrix of covariance given by the relation

$$W = \frac{1}{M} \sum_{m=1}^{M} \sum_{i=1}^{I} (y_{m,i,k} - y_{m,k})^{\mathrm{Tr}} (y_{m,i,k} - y_{m,k}), \tag{12}$$

$y_{m,i,k}$ denoting the k-th parameter of the i-th repetition of the m-th speaker, and

$$y_{m,k} = \frac{1}{I} \sum_{i=1}^{I} y_{m,i,k}. \tag{13}$$

2.4. *Experiment.* The strategy of the performed experiment is shown in Fig. 4.

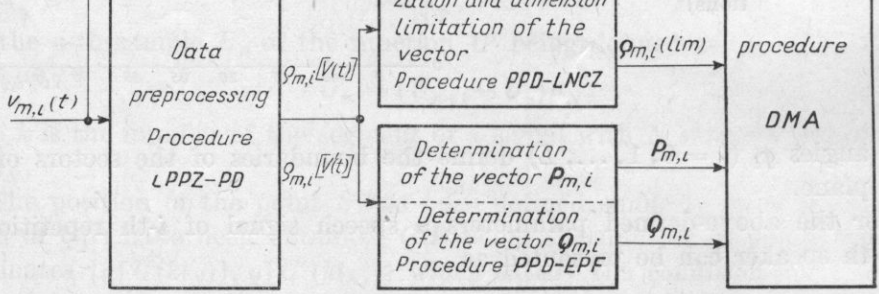

Fig. 4. The strategy of the identification experiment

The speech material for the experiments was provided by statements made by 20 male speakers of age 19-30. The statement of the speakers were recorded in two sessions A and B separated by a 3-month time interval. In the course of each session 5 repetitions of the key word were recorded. The speech signal was recorded on magnetic tape AN-25 by means of MDU-26 microphone and MP-224 tape recorder. The signal used for further processing had a S/N ratio of about 40 dB and frequency range 75-5000 Hz. For the conversion of the signal into a digital form enabling the extraction of parameters the recorder 7502 was used. The adopted threshold level was −35 dB in relation to the peak value of the signal and the sampling frequency was 10 kHz. The distributions of intervals $y_{m,i}$ were determined by means of the SEGDIG program [2].

The extraction of parameters obtained on the basis of the density of zero-crossings was realized in two stages.

The first stage involved the preliminary processing of data to determine the instant values (coordinates) of the density $\varrho[U(kt_N)]$ and $\varrho[U'(kt_N)]$ with $t_N = 20$ ms.

The second stage comprised the "curtailment" of the sequence $\varrho[U(kt_N)]$ to $K = 25$ elements, the time normalization of $\varrho[U(kt_N)]$ and $\varrho[U'(kt_N)]$ for $K = 25$ (cf. [5]) and the formation of vectors $\boldsymbol{P}_{m,i}$ and $\boldsymbol{Q}_{m,i}$ for $L = 4$ and 8. The extreme values of the angles φ_l were selected in the following manner:

$$\varphi_l = -\pi + \frac{2\pi}{L} l, \quad l = 0, 1, \ldots, L. \tag{14}$$

All sets of parameters described in this paper provide the basis for the formation of reference sequences and sequences to be identified. The reference sequences were obtained from statements recorded in session A; the sequences to be identified were obtained in both sessions A and B.

The results of voice identification with account for the technical data of parameters and the type of the sequence to be identified are shown in Table 1.

The results of voice identification indicate that the accuracy of the recognition depends considerably on the method used for the description of individual features.

The best results were obtained for the distribution of time intervals $\boldsymbol{y}_{m,i}$. In view of a not too large dimension K of this vector and no need for the time normalization, the priority should be given to this approach as being convenient and effective for the description of the reference pattern of voice obtained by the ZCA-method. The worse results were obtained for the sets $\boldsymbol{\rho}_{m,i}$ and $\boldsymbol{Q}_{m,i}$. Furthermore, prior to the formation of reference patterns and the patterns to be identified, the dimension of the set $\boldsymbol{\rho}_{m,i}$ must be reduced to the constant value K by normalization of "curtailment". The set $\boldsymbol{Q}_{m,i}$ for the adopted two

Table 1. Summary of the results of correct voice identification (in %)

Vector of parameters	Identified sequence from session *A*	from session *B*
$\boldsymbol{y}_{m,i}$ $K = 16$	92	78
$\boldsymbol{\rho}_{m,i}$ $K = 20$ (normalized)	90	72
$\boldsymbol{\rho}_{m,i}$ $K = 20$ (unnormalized)	89	68
$\boldsymbol{P}_{m,i}$ $L+2 = 6$	60	39
$\boldsymbol{P}_{m,i}$ $L+2 = 10$	63	49
$\boldsymbol{Q}_{m,i}$ $L+2 = 6$	77	48
$\boldsymbol{Q}_{m,i}$ $L+2 = 10$	84	61

dimensions of the vector $L+2$ is less efficient; for $L+2 = 10$ a considerably higher probability of correct identification was obtained and this gives evidence of the influence of the number of sectors of the phase plane on the results of identification for this set of parameters. Similar relations apply to the set $\boldsymbol{P}_{m,i}$ for which the least accurate results of identification were obtained.

For all sets of parameters a considerably smaller probability of correct identification in the case of sequences to be identified taken from session *B* was obtained, thus supporting the hypothesis of a pronounced effect of time lapse upon individual features of voices [1, 3].

On the basis of the results obtained it can be concluded that the ZCA--method can be effectively used for the formation of the sets of parameters discriminating the speakers in a short term analysis, provided a suitable method for the description of individual features of voice is used.

References

[1] B. S. Atal, *Automatic recognition of speakers from their voices*, Proceedings of IEEE, **64**, 4 460-475 (1976).

[2] C. Basztura and W. Majewski, *The application of long-term analysis of the zero-crossings of a speech signal in speaker automatic identification*, Archives of Acoustics **3**, 1 (1978).

[3] R. Gubrynowicz, *Problem of the recognition of individual features of voice*, Prace IPPT PAN, 28 (1969) (in Polish).

[4] — *Zero-crossing method in the analysis of a speech signal and automatic recognition of a limited set of words*, Prace IPPT PAN, 37 (1974) (in Polish).

[5] A. PAWLAK, C. BASZTURA and W. MAJEWSKI, *Time normalization of a statement in the process of speaker identification*, Proceedings of 24. Opened Seminar on Acoustics, Gdańsk-Władysławowo, September 1977, 84-87 (in Polish).

[6] M. SAMBUR, *Selection of acoustic features speaker identification* IEEE, **ASSP 23**, no. 2, 176-182 (1975).

[7] D. A. WASSON and R. DONALDSON, *Speech amplitude and zero-crossings for automated identification of human speakers* IEEE, **ASSP 23**, 390-392 (1975).

Received on 28th December 1977

ARCHIVES OF ACOUSTICS
3, 3, 197-210 (1978)

HYPOTHESIS OF COINCIDENCE OF SHEAR STRESSES IN THE EXCITATION OF HAIR CELLS

ANTONI JAROSZEWSKI

Laboratory of Musical Acoustics, Academy of Music, 00-368 Warszawa, Okólnik 2

A new hypothesis of neuromechanical "sharpening" in the cochlea inferred from the available morphological data and from the geometry of the distribution of stereocilia in OHC in relation to the distribution of shear stresses as determined by Tonndorf and by the author on cochlear models is presented.

Introduction

An idea of lateral suppression or "sharpening" in the perception of pitch was created in its simple form as a result of discrepancy between Helmholtz's theory [15] and the experimental observations. Helmholtz, investigating the perception of transients in musical sounds, reasoned that the mechanical frequency analyzing system in the form of basilar membrane must be damped in quite a significant degree. There was hence obvious contradiction arising from the necessity to assume high selectivity of the analyser to tally with its high pitch discrimination and from the observations which indicated its considerable damping.

A concept, well known as Gray's theory [12], introduced important modification of the Helmholtz theory and by the assumption that only these hair cells which receive the strongest excitation determine the pitch perception, was undoubtedly the first approach to what is presently termed as "sharpening" or lateral suppression. Almost 50 years later Hartline [13] discovered the phenomenon of inhibition of activity in visual receptors in the Limulus eye. This discovery was successfully used by Békésy [3] to refine earlier hypotheses pertinent to the nature of sharpening in the perception of pitch and based on the well-known observations by Mach.

Over the last decade or so the operation of lateral suppression or neural sharpening was considered as a logical consequence of data disparity resulting from the comparison of travelling wave envelopes in the BM with values of DL for frequency (Nordmark [31], Rakowski [32], Verschuure [42]) or with

selectivity of tuning curves representing the bioelectrical activity in single fibers of the eighth nerve (Kiang [25]), though in the latter case the differences are smaller.

It can be observed that travelling wave envelopes obtained by Békésy [1], which are frequently referred to, represent nothing but a first approximation of the true pattern because of the limits imposed by the method he used, i.e. direct visual examination with the use of an optical microscope with relatively low resolving power. For that reason he had had to use sound pressure levels reaching 140 dB, delivered to the tympanic membrane, to obtain sufficiently large amplitudes in the basilar membrane. At such pressure levels nonlinear processes are likely to occur at least in the region of the top of the travelling

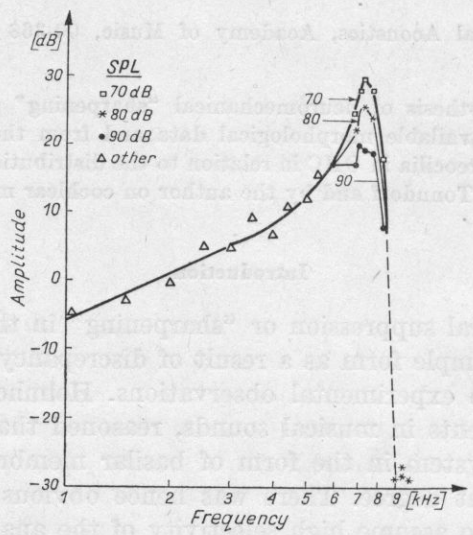

Fig. 1. Tuning curve of basilar membrane, after [33]

wave pattern (Fig. 1) which leads to its flattening (Rhode [33]). The possibility of occurrence of this artefact was also raised by Johnstone and Taylor [21]). They also point out that additional artefacts could have been involved as a result of observation of BM through the Reissner membrane practiced by Békésy and also from the use of post-mortem or proximatus post-mortem samples. However, similar comparisons with the newer results of the investigations of hydrodynamical tuning curves by Kohllöffel [26], which were obtained at excitation levels of approx. 70 dB SPL and using laser light, or of investigations by Rhode [33], Johnstone and Boyle [20] and Johnstone and Taylor [21], in which Mössbauer method (absorption of gamma irradiation) was used at abt. 70 to 90 dB SPL, also show considerable discrepancies with neurophysiological tuning curves and hence call for retaining of the assumption of locus of sharpening to some degree at cochlear level.

Aside of these considerations it can be observed that direct comparison between the envelopes of travelling wave in BM and neurophysiological tuning curves or else a search for direct correspondence between the selectivity of the travelling wave envelopes and the DL for frequency or the selectivity of psychoacoustical tuning curves can be regarded only as exaggerated simplification or misrepresentation. This understanding, however, was fairly widely accepted, e.g. after Davis [7] "each fibre has its "best" frequency but optimum is not sharp. The region of activity, as can be expected, corresponds with the travelling wave envelope". This simplification is likely to result from the uncertainty with regard to the mechanism of excitation or stimulation of hair cells, which leads to their depolarization. For this very reason the comparison of the travelling wave envelope normal to the BM surface and along its long axis with the tuning curves (neural) can be acceptable only as a first approximation.

As it can be learned from the literature a number of various concepts pertaining to the "sharpening" of cochlear selectivity on mechanical or hydromechanical basis or else on the assumption of both neural and hydromechanical processes in "sharpening" have been proposed (Tonndorf [40], [41], Zwicker [46]). There were also attempts to assign the neural "sharpening" to the multiple differentiation at various levels of auditory pathway (Huggins, Licklider [17], Dolatowski [8], Engström [9]). Ideas of different kind, presented by Zwislocki [47, 48], are based on the assumption of phase opposition in the activity of the populations of inner and outer hair cells. This phase opposition in bioelectrical activity of IHC and OHC was found by Zwislocki in the kanamycine-treated samples. This drug has a destructive influence mostly on IHC in the basal turn of the cochlea and mostly on OHC in the apical turn. The neural tuning curve obtained from these experiments at frequency of 5 kHz (a result of subtraction of tuning curves for IHC and OHC populations) is in its top comparable with that determined by Rhode [33] (flat top) and outside this region close to the tuning curves obtained by Kiang [25]. It is like an equivalent of Kiang's tuning curves particularly with respect to the slopes of the upper and lower flank, though delivered from the different experimental method. However, Zwislocki's theory of phase opposition, at least presently, does not seem to be fully and sufficiently documented, especially with regard to the kanamycin influence on both populations of hair cells.

Hydrodynamics of the cochlea

The stapes movement in the oval window results in a travelling wave in cochlea. From Tonndorf [40, 41] experimental works on cochlear models or works by Lesser and Berkley [28] it appears that the travelling wave is trochoidal in its nature, i.e. such a wave in which particles of the liquid medium move along elliptical or circular orbits. Closer examination reveals that particle tracks under certain conditions are even more complicated.

It can be observed that the trochoidal wave field is vectorial and three--dimensional generally, for instance for the case of a surface radial wave. Tonndorf [41], in his considerations pertaining to the hydrodynamics of cochlear models, assumes the two-dimensional field only and concludes that the existence of a trochoidal wave, the similarity of waves in the medium and in BM and also the decrease of the field vector perpendicular to the BM surface with distance, seem to indicate that the movement of liquid medium in the cochlea accompanied byy the BM deformations well resembles Lambs surface waves. It seems likely that this simplification assumed for clarity of dynamical representation of the system behaviour is not pertinent in regard to Tonndorf's observations of the distribution of shear stresses in BM (or between the tectorial and basilar membranes) performed on cochlear models. These observations seem to indicate for the existence of a three-dimensional vectorial field in the cochlear medium.

The latter observations are extremely interesting from the point of view of Tonndorf's [41] and Zwicker's [46] concepts about the mechanical or hydromechanical nature of the "sharpening" process. The envelope of a travelling wave, longitudinal shear stresses and radial shear stresses, as measured by Tonndorf [41] on cochlear models, are presented in Fig. 2. Tonndorfs tates that "these mechanical transformations may be dominant if not the only factors determining the "sharpening" observed in neurophysiological activity", though he does not disregard the possibility of neural processing.

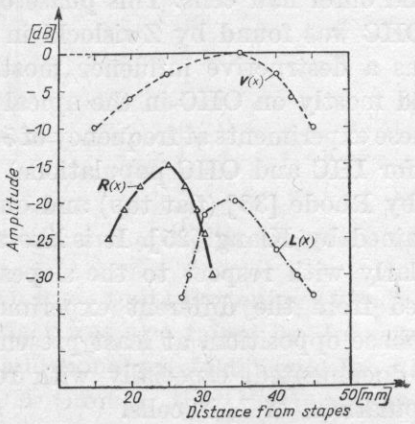

Fig. 2. Shear stresses in the cochlear model, after [41]

It must be, however, stressed in that context that the envelopes of both longitudinal and radial shear stresses, though characterized by better selectivity with respect to the normal deflection travelling wave, are far from the selectivity of neurophysiological tuning curves, particularly their portions close to CF's. Nevertheless, Tonndorf's data [41] on shear stresses in the cochlear models and their redetermination by the autor are, as it seems, the only data available.

Neurophysiological data

The available data practically rule out the possibility of excitation of hair cells through axial stresses, i.e. along the axis of stereocilia exerted by the normal pressure as it was necessary in the so-called "heavy beam theory" by Huggins and Licklider [17]. Békésy's data [2] from the early simple experiments using vibrating needle show that evidently hair cells are mostly sensitive for the stimulation tangential to the BM surface. Hence it is postulated [9] that stereocilia rather perform like levers and behave passively transferring the energy of shear stresses from the tectorial membrane to the basal body. Basal body, according to Engström, should be identified as main element which under stimulation leads to the depolarization of the hair cell.

Basic morphological data concerning both hair cells populations are derived from Held [14] and Kolmer [27]. More recent data by Flock et al. [11], Engström et al. [9] and, particularly, these by Spoendlin [36, 37] supply a vast amount of morphological information; with respect to the mechanism of hair cells stimulation, however, the ideas revealed by these authors seem to have comparatively little in common. Thus Flock et al. postulate radial shear stresses as leading to the depolarization of hair cells, whereas Engström et al. maintain that radial shear can be regarded as the main stimulating factor only with respect to the inner hair cells because of the simple isotropic geometrical configuration of stereocilia of these cells. Again Flock et al. pointa out very characteristic configuration of stereocilia in the outer hair cells in all the three rows resembling "W" to some extent (Fig. 3). This very special arrangement according to Flock et al. (1962) indicates that the sensitivity of OHC is increased in some priviliged directions. These directions of increased sensitivity should correspond

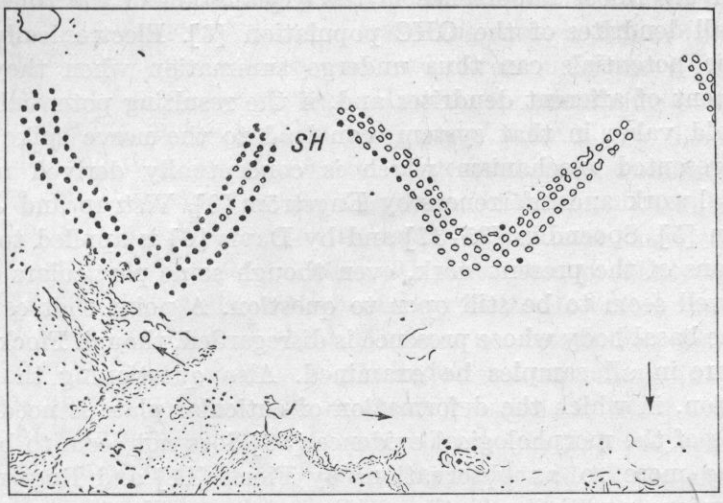

Fig. 3. Arrangement of stereocilia in OHC, after [11]

with oblique radial and longitudinal shear stresses or, in other words, the OHC should demonstrate some degree of directional sensitivity.

Spoendlin [36, 37], by inference from his morphological studies of Cortis' organ using an electron microscope, seems to deny the role of the basal body in the stimulation and eventually depolarization of hair cells since he was unable to find this structure in his samples except in very young animals and guinea pigs [11]. He also argues that the cuticular plate, in which stereocilia are anchored, is so stiff a structure that its deformation under lever action of stereocilia does not seem to be possible. Hence, the deformation of cuticular plate and the resulting stimulation of the basal body seems to be open to question.

A very interesting hypothesis with reference to the initiation of the mechano-electrical transformation process was reported by Vistrup and Jensen [43] and Christiansen [5]. This hypothesis follows the observation of mucopolisaccharides which, under mechanical shear stresses, develop surface electric potentials. Mucopolisaccharides showing even some sort of regular structures were found in between the stereocilia spaces by Spoendlin [35]. The shear stresses which are present between the stereocilia, following stimulation of BM [41], could possibly lead to the initiation of such a reaction [36, 37]. The mechano-electrical transformation of that nature seems also to be in agreement with the observations by Tasaki and Spyropoulos [38] and Butler [4] from which it follows that Cortis' organ space without stimulation is isopotential.

Morphological data are also available which indicate the possibility of synaptic transition from the hair cell to the afferent nerve endings on the principle of the chemical process [36]. As a result of such a synaptic process, gradually growing postsynaptic potential is developed in nerve endings. This potential, characterised by the absence of the threshold values, may very likely be of uttermost importance in the explanation of the time summation process in all dendrites of the OHC population [6]. Electronically conducted postsynaptic potentials can thus undergo summation when they reach the initial segment of afferent dendrites and, if the resulting potential approaches the threshold value in that system, can lead to the nerve spike firing [36].

The presented mechanism which is conceptually derived mainly from experimental work and inferrences by Engström [9], Vistrup and Jensen [43], Christiansen [5], Spoendlin [35-37] and by Davis [6] is applied to the further considerations of the present work, even though some particulars of that concept may well seem to be still open to question. A point that can be argued concerns the basal body whose presence is disregarded, though Flock [11] found this structure in all samples he examined. Also questioning the mechanism of stimulation, in which the deformation of cuticular plate is needed [9], only on the basis of the morphological evidence [36] does not seem to be quite convincing, the more so as observations by Flock [11] and Engström [9] and their conclusions pertaining to the rigidity of stereocilia were not questioned, though it could well have been of advantage for Spoendlin's [36] hypotheses.

It can be learned that mucopolisaccharides were found by Spoendlin between the stereocilia, if not along the whole length, then at least at some definite length. Hence, with the assumption of considerable rigidity of both, the stereocilia and the cuticular plate, it appears to be rather difficult to explain in what a way the shear stresses between the stereocilia can be developed, necessary for the graded potential to appear. Once the complete rigidity of cuticular plate is assumed, the shear stresses between the stereocilia can develop only if the latter undergo bending. However, this concept seems to be contradictory with respect to Spoendlin's finding which indicates that mucopolisaccharides occupy probably some considerable length of the stereocilia space. From classical mechanics it is known that a bending of stereocilia, anchored in the rigid cuticular plate, would take place chiefly if not only in the vicinity of anchored ends. In such a case the presence of mucopolisaccharides outside this small fraction of stereocilia length would appear to be rather a sort of unfounded. Therefore it seems not to be improbable that Spoendlin's inferrences with regard to the rigidity of cuticular plate, which are in contrast with Engström's [9] implications, are wrong. If that was true, and assuming a considerable degree of stiffness in stereocilia, shear stresses would occur at the whole or at the large part of stereocilia length. On the other hand, the assumption of elastic cuticular plate seems to make Spoendlin's argument with regard to Flock [11] and Engström [9] unsound. Summing up it appears that the available empirical data are inconsistent, as are the theories built up thereupon.

Psychoacoustical data and locus of sharpening

A comparison between the neurophysiological tuning curves obtained at the 8-th nerve level and the envelopes of travelling wave in BM or the envelopes of radial or longitudinal shear stresses may lead to reasoning that the sharpening at this level takes place in the cochlea. Hypotheses pertaining to the hydromechanical sharpening in the cochlea were given after all by Tonndorf [40] and Zwicker [46] and they are not new in the general sense. Tonndorf indicates the possibility of sharpening resulting from mechanical transformations of normal deflection of BM to the radial and longitudinal shear stresses and suggests after Lowenstein and Wersäll [29] that most probably only radial stresses are engaged in the stimulation of hair cells. However, the envelopes of both radial and longitudinal shear stresses, as determined by Tonndorf, diverge significantly from the neurophysiological tuning curves [25], particularly, as it was already pointed out, in the top region. It can be shown that with respect to neurophysiological tuning curves [22-25] the selectivity of hydrodynamical tuning curves [20, 21, 26, 33], expressed by the slopes of the flanks of TC, is worse by the ratio of 1 : 2 to 1 : 4 and still worse in the top of the curve region.

The results of investigations of psychoacoustical tuning curves [18, 19, 44], which show that the slopes of the upper flank of tuning curves in the top region reach from 10^3 to $2.5 \cdot 10^3$ dB/oct, seem to point out quite soundly that the process of "sharpening" is not completed at the primary neurons level because the slopes of neurophysiological tuning curves at the eighth nerve level are considerably lower [10, 25, 45].

Hypothesis of coincidence of shear in hydrodynamical sharpening

According to Engström et al. [9] the izotropic distribution of stereicilia in IHC suggests that IHC are stimulated only by radial shear stresses. On the contrary, Tonndorf [41] by the analysis of the role of tectorial membrane comes to the conclusion that IHC can be stimulated but only by longitudinal shear stresses. Similar implications were formulated also by Spoendlin [36]. In spite of the lack of sufficient and convincing experimental data it seems likely that IHC at any rate may demonstrate either unidirectional characteristic of sensitivity or, which seems even more probable, have the same sensitivity for shear stresses from any direction (tangential shear). This is not quite in agreement with findings by Spoendlin [36, 37] who was able to show some anizotropic arrangement also in IHC.

The very peculiar distribution of stereocilia in OHC does not seem to permit for the assumption of the analogical hypothesis because in nature rarely structures can be found in which complication would be purposeless. If the structure of OHC and, particularly, the distribution of stereocilia very close in shape to the letter "W" with low tooth in the middle and limbs at approximately 45° to the length of BM is estimated, it seems very likely that the priviledged directions of stimulation may be oblique. In that case OHC would be particularly sensitive or sensitive only for shear stresses oblique with respect to the direction of travelling wave propagation.

Spoendlin [36], discussing the nature of the graded postsynaptic potential development, states that the deformation of the inter-stereocilia mucopolisaccharide molecular structures (and hence the accompanying electrical reaction) is the largest if the rows of stereocilia are parallel to the direction of bending and the smallest if the rows of stereocilia are perpendicular to that direction. Even with the assumption that stereocilia do not undergo bending (as Spoendlin did assume) but only deflection near their place of anchorage, i.e. cuticular plate — which depends, as discussed above, on the relative stiffness of both stereocilia and cuticular plate which can not be determined yet with the sufficient certainty — the principle of directional sensitivity of OHC with their anizotropic stereocilia configuration can well seem true. In case of rather stiff stereocilia and relatively elastic cuticular plate, possibly only over the portion close to the anchorage of hairs, the graded potentials would develop in the whole interstereocilia mucopolisaccharide molecular structures. In spite of the ob-

vious possibility of this reasoning, Spoendlin [35, 36] does not cease from the well accepted and popular assumption that the priviledged directions in sensitivity characteristics of OHC and IHC are radial and longitudinal, respectively.

It is easy to observe that oblique shear stresses appear solely in the region of coincidence of both longitudinal and radial shear stresses, as they were determined by Tonndorf [41] and by the author (this report). There is only a relatively limited region, in terms of BM length in which these two kinds of shear occur together. This region that has been termed the "region of coincidence" is, contrary to the envelopes of travelling wave, longitudinal shear stresses and radial shear stresses, comparatively narrow in the frequency domain. So, if the presented hypotheses and reasoning would gain more experimental evidence and support, particularly by the determination of directional characteristics of OHC sensitivity, then they could be significant in the understanding of the sharpening phenomena at cochlear level and of the pitch perception as well. Thus, assuming that the depolarization of the basal body or the growth of graded potential at the initial dendrites of afferent fibers takes place only for the oblique shear stresses, then this activity would result from the shear determined by the difference of vectors $\boldsymbol{R}(x)$ and $\boldsymbol{L}(x)$. Functions $\boldsymbol{R}(x) - \boldsymbol{L}(x)$, derived from Tonndorf's [41] data and from the own data obtained on 10 : 1 scale cochlear model, are presented in Figs. 4 and 5. The quantitative differences between the two sets of data do not seem to be alarming as obtained from the seemingly different models and most probably also procedures. An important

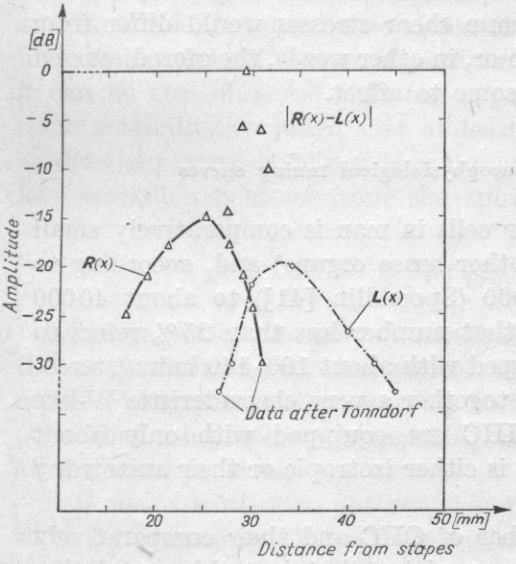

Fig. 4. Region of coincidence of shear stresses in cochlear model calculated from the data by Tonndorf [41]

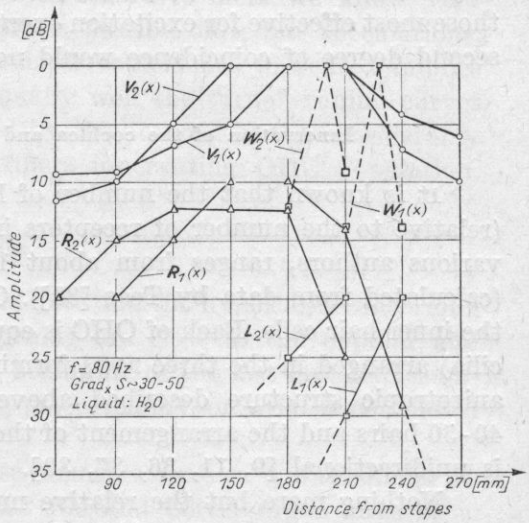

Fig. 5. The distribution of shear stresses in the cochlear model. Two membranes with different elasticity and thickness $W(x)$ – the coincidence functions of $R(x)$ and $L(x)$

detail in the concept of coincidence of shear stresses in the stimulation of hair cell is that within one full period of stimulation, in the top region of the $R(x)-L(x)$ curve, i.e. where scalar values of both vectors are equal, the phase of $R(x)$ vector changes by 180°. Hence, the stereocilia in the limbs of "W-like" configuration are subjected to the shear forces $F(x)$ of equal amplitude but inclined 45° and −45° with respect to the BM length.

Now then the next or second degree of coincidence occurs which can be considered as the proper coincidence and which results from the action of equal amplitude but directed along the rows of stereocilia in OHC vectors of shear stresses (i.e. 90° aside one from the other). It can be that only and solely that coincidence, which can be found nowhere but at the top of $R(x)-L(x)$ function, is associated with the depolarization of the basal body or assuming different mechanism, the growth of the graded potential in the initial dendrites of afferent network, eventually resulting in firing of the nerve spike if the characteristic threshold value was reached.

Approval of the mechanical transformations after Tonndorf [41] and assumption of the operation of sharpening according to the principle of the hypothesis of coincidence may include, in their nature, explanation for the existence of excitatory and inhibitory areas. Namely, if the envelopes of shear stresses overlap each other, some kind of blocking of at least a fraction of OHC population is likely to occur on both sides of $R(x)-L(x)$ maximum. Such blocking could be expected as a result of prevalence of the radial shear vector on one side and the longitudinal shear vector on the other side of excitatory area. In that way on both sides of $R(x)-L(x)$ maximum shear stresses would differ from those most effective for excitation exertion or, in other words, the aforediscussed second degree of coincidence would not come to effect.

Innervation of the cochlea and neurophysiological tuning curves

It is known that the number of hair cells in man is comparatively small (relative to the number of receptors in other sense organs) and, according to various authors, ranges from about 15000 (Spoendlin [41]) to about 40000 (calculated from data by Teas [39]). Of that number less than 25 % refers to the inner hair cells. Each of OHC is equipped with about 100-140 hairs (stereocilia) arranged in the three rows forming together a very characteristic W-like anizotropic structure described above. IHC are equipped with only about 40-50 hairs and the arrangement of them is either izotropic or their anizotropy is unidirectional [9, 11, 36, 37, 39].

Nothing more but the relative number of OHC and their comparatively complicated anizotropy could lead to the suspicion that just this population should demonstrate higher discriminatory ability relative to the IHC population. Contradictory argumentation could be performed using morphological data pertinent to the number of the afferent links; only about 3000-4000 of those

innervate the whole population of OHC whereas the most afferents, i.e. about 50000, carry information from the IHC.

Aditionally the IHC have afferent connections almost entirely with the radial fibers whilst the connections of OHC dendrites with afferent network are accomplished by the external spiral fibers, which connects with groups of OHC, covering some considerable space. These reasons seem to have led Spoendlin [36] to the assumption that inner hair cells are dominant in the discrimination of pitch.

It seems that this assumption can be regarded as quite logical from the point of view of morphological evidence but there are also some other aspects which may indicate that it as well can be recognized as doubtful and formulated without sufficient insight into functional evidence.

One of the doubtless facts, which can be used in this argument, follows from the relative number of afferent neurons associated with the OHC and IHC. As it was mentioned, only about 5% of neurons within the eighth nerve are afferents carrying information from OHC. Hence, it well can be that practically all the records of bioelectrical activity, as obtained by Kiang [25] and others, could be pertinent to the radial fibers belonging to IHC population. From that point of view it may seem probable that the neurophysiological tuning curves, obtained by Kiang at the 8-th nerve level and widely accepted as the determinant of the frequency selectivity of the auditory pathway at that level, may turn out not to be actually "true" tuning curves as they may reflect the activity of only IHC population. Whatever we will learn about the activity of OHC and their role, it must be admitted that with regard to facts we know very little at present. However, if nothing more is possible now but speculations, it can be also observed that the hypothesis of coincidence presented implies some possibility to judge that at least equally well the "true" tuning curves at the eight nerve level can be represented by the activity in the considerably less accessible neurons from the spiral fibers innervating OHC population.

Conclusion

The presented and quoted experimental data and the hypothesis concerning the mechanism of neuromechanical sharpening are close to the popular and rather widely accepted, at least up to the beginning of the last decade, assumption that the process of sharpening takes place mainly or even is completed at the cochlear level.

It seems worthy to observe that these concepts were in a way similar to those by Helmholtz [15] who declared that BM and Cortis' organ have basic role in the perception of pitch, though his ideas pertaining to the nature of analysis at that level were quite naturally very simple.

The presented in this report hypothesis of coincidence of longitudinal and radial vectors of the field of shear stresses in the travelling wave demonstra-

tes still further effort to explain the unbelievably high selectivity of the ear analyzer, even as low as at the cochlear level. Assuming that Kiang's [25] tuning curves (in spite of the former criticism) reflect that selectivity to some degree at least, it comes to about 200 dB/oct at 1 kHz as expressed by the upper flank slope [10, 45]. Nevertheless it is by an order of magnitude lower than the selectivity in the psychoacoustical tuning curves reported in the papers cited [18, 19, 44].

The presented data seem to support the place theory. However, it should be stressed that essentially the spatial data do not contradict the temporal data (time theory) and to prove such contradiction was by no means intended by the author. It can also be noticed that the travelling wave theory, though it cannot be questioned in the face of the available experimental data both hydrodynamical and neurophysiological, still offers many problems yet unsolved in detail.

Undoubtedly the data by Hind et al. [16] and also by Rose and al. [34], which show that the regions of activity in terms of frequency at the eighth nerve level evoked by sine signals at from 20 to 100 dB SPL, correspond with considerable regions (dimensionally) in the basilar membrane add to the complexity of pitch perception process. On the other hand, it may seem possible, particularly with morphological data and inferrences by Spoendlin [37] at hand, that the mentioned apparent complications result from the misleading interpretation of the up-to-date available neurophysiological data. In one of his papers Spoendlin expressed his doubts in the statement that "Kiang probably recorded mainly from the neurons associated with IHC and his results reflect the mechanism of IHC coding system".

It is also probable that similar objections may apply equally to the data by Hind [16] and Rose [34]. For that reason, with lack of the sufficiently documented data pertaining to the activity of OHC, any comparison between the slopes of neurophysiological tuning curves obtained heretofore and the slopes of psychoacoustical (or hydrodynamical) tuning curves can evoke quite substantial criticism. Nevertheless such comparisons are evidently popular [10, 30] in spite of that, as it was mentioned, there is actually very little known about the bioelectrical activity and the role which OHC population plays in the perception of pitch.

In this context, the presented hypothetical model of neuromechanical sharpening, working on the principle of common effect of both radial and longitudinal shear on the OHC with the assumption of directional sensitivity characteristics in this population, is an attempt to determine potential possibilities of OHC with respect to the discrimination of pitch. Some aspects of this hypothetical model are in agreement with Evans' [10] inferrences concerning the "second filter hypothesis", who wrote that it is highly probable that "each hair cell is equipped with a separate "private" second filter".

References

[1] VON BÉKÉSY, *Über die Schwingungen der Schneckentrennwand beim Präparat und Ohrenmodell*, Akust. **7**, 173-186 (1942).

[2] — *The psychology of hearing* in *The experiments in hearing*, Mc. Graw-Hill, New York 1960.

[3] — *Sensory Inhibition*, Princeton Univ. Press, Princeton 1967.

[4] R. A. BUTLER, *Experimental observations on a negative d.c. resting potential in the cochlea*, J. Acoust. Soc. Am, **36**, 1016 (A), 1964.

[5] J. A. CHRISTIANSEN, *On hyaluronate molecules in the labyrynth as mechano-electrical transducers and as molecular motors acting as resonators*, Acta Oto-Laryngol., **57**, 33-49 (1964).

[6] H. DAVIS, *Some principles of sensory receptor action*, Physiol. Rev., **41**, 391-416 (1961).

[7] — *Neurophysiology and neuroanatomy of the cochlea*, J. Acoust. Soc. Am., **34**, 1377-1385 (1962).

[8] W. A. DOLATOWSKI, *Elements of dynamics of processes in the auditory receptor*, Archi-, wum Akustyki, **3**, 11-20 (1969) (in Polish).

[9] ENGSTRÖM et al., *Structure and functions of the sensory hairs of the inner ear*, J. Acoust. Soc. Am., **34**, 1356-1363 (1962).

[10] E. F. EVANS (1975), *The sharpening of cochlear frequency selectivity in the normal and abnormal cochlea*, Audiology, **14**, 419-422 (1975).

[11] A. FLOCK et al., *Morphological basis of directional sensitivity of the outer hair cells in the organ of Corti*, J. Acoust. Soc. Am., **34**, 1351-1355 (1962).

[12] A. A. GRAY, *On a modification of Helmholtz's theory of hearing*, J. Anat. Physiol. Lond., **43**, 324-350 (1900).

[13] H. K. HARTLINE (1949), *Inhibition of activity of visual receptors by luminating nearby retinal areas in the Limulus eye*, Fed. Proc. **8**, 69 (1949).

[14] H. HELD, *Die Cochlea der Säuger und der Vögel*, Handbuch der normalen und pathologischen Physiologie, Springer, 1926.

[15] H. VON HELMHOLTZ (1863), *Die Lehre den Tonempfindungen als physiologische Grundlage für die Theorie der Musik*, F. Vieweg u. Sohn, Braunschweig 1863.

[16] J. E. HIND et al., *Two-tone masking effects in squirrel monkey auditory nerve fibers*, in *Freguency analysis and periodicity detection in hearing*, R. Plomp and G. F. Smoorenburg Eds. Sijthoff, A. W., The Netherlands, 195, 1970.

[17] W. H. HUGGINS and J. C. R. LICKLIDER, *Place mechanisms of auditory frequency analysis*, J. Acoust. Soc. Am., **23**, 290-299 (1961).

[18] A. JAROSZEWSKI and A. RAKOWSKI (1976), *Psychoacoustical equivalents of tuning curves obtained using post-stimulatory masking technique*, Archives of Acoustics., **1**, 2, 127-135 (1976).

[19] A. JAROSZEWSKI, *A new method for determination of frequency selectivity in post-stimulatory masking*, H-40, 9-ICA, Madrid (Acoustica, in print) (1977).

[20] B. M. JOHNSTONE and A. J. F. BOYLE, *Basilar membrane vibrations examined with the Mössbauer technique*, Science, N. Y., **158**, 389-390 (1967).

[21] B. M. JOHNSTONE and K. TAYLOR, *Mechanical aspects of cochlear function*, in *Frequency analysis and periodicity detection in hearing*, R. Plomp and G. F. Smooreburg, Eds. Leiden, A. W. Sijthoff, 1970.

[22] Y. KATSUKI, N. SUGA and Y. KANNO (1962), *Neural mechanisms of the periferal and central auditory system in monkey*, J. Acoust. Soc. Am., **34**, 1396-1410 (1962).

[23] N. Y. S. KIANG, T. WATANABE, E. C. THOMAS and L. F. CLARK, *Discharge patterns of single fibers in the cats auditory nerve*, Res. Mon., No 35, MIT Press, Cambridge, Mass. (1965).

[24] N. Y. S. KIANG, M. B. SACHS and W. T. PEAKE, *Slopes of tuning curves for single auditory nerve fibers*, J. Acoust. Soc. Am., **42**, 1341-1342 (1967).

[25] N. Y. S. KIANG, *Stimulus coding in the auditory nerve and cochlear nucleus*, Acta Oto-Laryngol., **59**, 186-200 (1965).

[26] L. V. E. KOHLLÖFFEL (1972), *A study of basilar membrane vibrations, II. The vibratory amplitude and phase patern along the basilar membrane*, Acoustica, **27**, 66-81 (1972).

[27] W. KOLMER, *Gehörorgan*, Handbuch der mikroskopischen Anatomie des Menschen, Springer, 1927.

[28] M. B. LESSER and D. A. BERKLEY (1972), *Fluid mechanics of the cochlea*, Part 1, J. Fluid Mech. **51**, 3, 497-512 (1972).

[29] O. LÖWENSTEIN and J. WERSÄLL, *A fundamental interpretation of the electron microscopic structure of the sensory hairs in the cistae of the elasmobranch raja clavata in terms of directional sensitivity*, Nature, **184**, 1807-1018 (1959).

[30] A. R. Møller, *Coding of sounds in lower levels of the audiatory system*, Quart. Rev. Bioph., **5**, 59-155 (1972).

[31] S. O. NORDMARK, *Mechanism of frequency discrimination*, J. Acoust. Soc. Am., **44**, 1533-1540 (1968).

[32] A. RAKOWSKI, *Pitch discrimination at the thershold of hearing*, 7th ICA, Budapest, 20-H-6, 1971.

[33] W. S. RHODE, *Observations of the vibration of the basilar membrane in squirrel monkey using the Mössbauer technique*, J. Acoust. Soc. Am., **49**, 1218-1230 (1970).

[34] J. E. ROSE, D. J. ANDERSON and J. F. BRUGGE, *Some effects of stimulus intensity on response of auditory nerve fibers in the squirrel monkey*, J. Neurophysiol., **34**, 685-699 (1971).

[35] H. SPOENDLIN, *Ultrastructure and peripheral innervation pattern of the receptor in relation to the first coding of acoustic message*, in *Hearing mechanism in vertebrates*, A.V.S. de Rueck, J. Knight, Eds. Churchill, London 1968.

[36] — *Structural basis for peripheral frequency analysis*, in *Frequency analysis and periodicity detection in hearing*, R. Plomp, G. F. Smoorenburg, Eds. Sijthoff, Leiden 1970.

[37] — *Neuroanatomical basis of cochlear coding mechanisms*, Audiology, **14**, 383-407 (1975).

[38] J. TASAKI and C. S. SPYROPOULOS, *Stria vascularis as source of endocochlear potential*, J. Neurophysiol., **22**, 149-155 (1959).

[39] D. C. TEAS, *Cochlear processes*, in *Foundations of modern auditory theory*, J. V. Tobias, Ed., Academic Press, 1970.

[40] J. TONNDORF, *Time-frequency analysis along the partition of cochlear models: A modified place concept*, J. Acoust. Soc. Am., **34**, 1337-1350 (1962).

[41] — *Cochlear mechanics and hydrodynamics*, in *Foundations of modern auditory theory*, J. V. Tobias, Ed., Academic Press, 1970.

[42] J. VERSCHUURE and A. A. VON MEETEREN, *The effect of intensity on pitch*, Acoustica, **32**, 33-44 (1975).

[43] TH. VISTRUP and C. E. JENSEN, *Three reports on the chemical composition of the fluids of the labyrinth*, An. Otol. Laryngol., **63**, 151-163 (1954).

[44] L. L. M. VOGTEN, *Low level pure-tone masking and two-tone suppression*, IPO Annual Progress Raport, No 9, 22-31 (1974).

[45] O. WILSON, Discussion: B. M. JOHNSTONE and K. TAYLOR, Mechanical aspects of cochlear function, in *Frequency Analysis and Periodicity detection in hearing*, R. Plomp and G. F. Smoorenburg, Eds., A. W. Sijthoff, Leiden 1970.

[46] E. ZWICKER, *On a psychoacoustical equivalent of tuning curves*, in *Facts and models in hearing*, E. Zwicker, E. Terhardt, Eds., Springer Verlag, 1974.

[47] J. J. ZWISLOCKI, *A possible neuro-mechanical sound analysis in the cochlea*, Symposium on auditory analysis and perception of speech, Leningrad; Acustica, **31**, 354-359 (1974).

[48] — *Phase opposition between inner and outer hair cells and auditory sound analysis*, Audiology, **14**, 443-455 (1975).

Received on 17th October 1977

ARCHIVES OF ACOUSTICS
3, 3, 211-224 (1978)

IMPEDANCE OF THE UNBAFFLED CYLINDRICAL PIPE OUTLET FOR THE PLANE WAVE INCIDENT AT THE OUTLET*

ANNA SNAKOWSKA

Institute of Physics, Higher Pedagogical School
35-959 Rzeszów, ul. Rejtana 16a

The paper presents formulae for the impedance of the outlet of semi-infinite cylindrical wave-guide derived by considering the propagation of a plane wave and accounting for the generation of higher Bessel modes due to the diffraction at the opened end of the wave-guide. For this purpose expressions for the refraction and transformation coefficients of the basic mode were derived by solving exactly the wave equations with suitable boundary conditions using Wiener-Hopf factorization.

1. Introduction

In the practical applications of acoustics an important role is played by the phenomena occurring at the opened ends of wave-guides, e.g. of measuring pipes and acoustic horns. The first attempt to describe these phenomena was presented by Rayleigh [1] who had assumed uniform distribution of the velocity of vibrations at the outlet provided additionally with an infinitely rigid acoustic baffle. A further step towards the definition of the acoustic field inside the semi-infinite unbaffled cylindrical waveguide was made by Levine and Schwinger [2]. They assumed, however, that a basic mode plane wave propagates in the direction of the outlet and that because of diffraction at the opened end of the wave-guide only the plane wave with an amplitude described by the complex coefficient of reflection propagates. The impedance of the outlet calculated on the basis of the value of this coefficient is given, among others, by Żyszkowski ([3], p. 218). However, it is known, e.g. from the theory of the infinite cylindrical wave-quide (cf. [4]), that such assumptions are valid only when the diffraction parameter of the wave-guide, i.e. the product of the wave number and the pipe radius is smaller than the value of the zero-crossing of

* This paper is a contribution to the interdisciplinary problem MR.I.24

the Bessel function of the first order, equal to 3,8317... This model has thus a limited application to higher frequencies and larger diameters of the wave-guides.

In 1949 Wajnsztejn [6] developed an analytical theory of the acoustic field of a semi-infinite unbaffled cylindrical wave-guide utilizing the method of solution of a similar problem for electromagnetic waves [5]. Basing on his results the author of the present paper has calculated the impedance of the outlet of the unbaffled cylindrical wave-guide for the plane wave incident at the outlet with the aid of an exact solution of the wave equation for any value of the diffraction parameter. The result obtained can also be interpreted as an impedance of a circular sound source located at the bottom of a semi-infinite, rigid cylinder of the identical radius.

2. Solution of wave equation

Let us consider a cylindrical wave-guide with an infinite, thin and rigid wall and select a cylindrical coordinate system in which the Z-axis coincides with the symmetry axis of the wave-guide. The wave-guide wall Σ is given by the equation of the side-wall of the semi-infinite cylinder with a radius a:

$$\Sigma = \{(r, z): r = a, z \geqslant 0\}.$$

Let us assume further that the acoustic potential $\Phi(r, z)$ does not depend on angle φ and its dependence on time is described by the factor expressed in the form $\exp(-i\omega t)$. The wave equation for the potential has thus the following from:

$$\frac{1}{r}\left(r\frac{\partial \Phi}{\partial r}\right)+\frac{\partial^2 \Phi}{\partial z^2}+k^2\Phi = 0. \tag{1.1}$$

The assumption that the wave-guide is perfectly rigid leads to the boundary condition

$$\left.\frac{\partial \Phi}{\partial r}\right|_{\Sigma} = 0. \tag{1.2}$$

This means that the normal component of velocity vanishes at the wave-guide wall. The second boundary condition requires that the potential should be continuous at the surface extention in the negative direction of the Z-axis:

$$\lim_{r\to a_+} \Phi(r, z) = \lim_{r\to a_-} \Phi(r, z), \qquad z < 0. \tag{1.3}$$

The solution of the problem of acoustic field of the wave-guide consists in finding the function $\Phi(r, z)$ which satisfies equation (1.1) for the boundary conditions (1.2) and (1.3) and the Sommerfeld condition of radiation (cf. [4]).

Let us assume that the partial solution of this problem, depending additionally on a parameter w and modified by a function $F(w)$ is the solution obtained for the infinite wave-guide [5], [6]

$$\Phi(r,z,w) = i2\pi^2 v F(w) e^{iwz/a} \begin{cases} J_0\left(v\frac{r}{a}\right)[H_0^{(1)}(V)]', \\ [J_0(v)]' H_0^{(1)}\left(V\frac{r}{a}\right), \end{cases} \tag{1.4}$$

where

$$v = \sqrt{(ka)^2 - w^2}. \tag{1.5}$$

The upper product of cylindrical functions in braces refers to the interior of the cylinder described by Σ whereas the lower one to the outside of this cylinder, i.e. for $r > a$ [4].

The required potential $\Phi(r, z)$ is assumed to be a superposition of the above partial solutions [5], [6],

$$\Phi(r,z) = \int_C \Phi(r,z,w)\,dw, \tag{1.6}$$

where C is a contour which is selected so that the obtained solution satisfies the imposed boundary conditions. In particular, the boundary condition (1.2) now takes the form

$$\int_C e^{iwz/a} L(w) F(w)\,dw = 0, \qquad z > 0, \tag{1.7}$$

where

$$L(w) = \frac{\pi V^2}{a} J_1(v) H_1^{(1)}(v). \tag{1.8}$$

By calculating then the potential step on the surface $r = a$,

$$\Phi(a_+, z, w) - \Phi(a_-, z, w) = 4\pi F(w) e^{iwz/a}, \tag{1.9}$$

it is possible to write the boundary condition (1.3) in the form

$$\int_C e^{iwz/a} F(w)\,dw = 0, \qquad z < 0. \tag{1.10}$$

Finding the potential $\Phi(r, z)$ is thus reduced to the determination of such a function $F(w)$ and a contour that equations (1.7) and (1.10) are satisfied. The solution of these equations can be obtained by the Wiener-Hopf method, by factorizing analytically integrands $L(w)$ and $F(w)$ into factors $L_+(w)$ and $L_-(w)$ in the and lower half-plane of the complex variable w, respectively, as this permits to make use of the convolution theorem [7].

A further development of the factorization method, described extensively, among others, in papers [5] and [6], leads to the following expression for the acoustic potential of the wave-guide under consideration:

$$\Phi(r, z) = -A\left[e^{-ikz} + \sum_{n=0}^{\infty} R_n \frac{J_0\left(\mu_n \frac{r}{a}\right)}{J_0(\mu_n)} \cdot e^{i\gamma_n \frac{z}{a}}\right], \tag{1.11}$$

where R_n is the coefficient of transformation of the incident wave into the n-th wave mode with a wave number γ_n/a, with

$$\gamma_n = \sqrt{(ka)^2 - \mu_n^2}, \tag{1.12}$$

and μ_n is the n-th zero-crossing of the Besel function of the first order

$$J_1(\mu_n) = 0.$$

The first component in square brackets represents the plane wave which, according to the assumption, propagates in the direction of the wave-guide outlet and is transformed there into an infinite number of waves with a Bessel distribution which propagate in the opposite direction. Analyzing carefully the exponential expressions under the sum sign we see that for a fixed diffraction parameter only a certain number of components will represent the waves which can propagate along the wave-guide, since, if the condition

$$ka = \varkappa > \mu_n \tag{1.13}$$

is satisfied, the exponent of the exponential function will be an imaginary number. Starting, however, from a certain N such that

$$\mu_N < \varkappa < \mu_{N+1}, \tag{1.14}$$

the exponents will be negative real numbers and thus the corresponding components of the sum will represent a disturbance, attenuated exponentially with increasing coordinate Z. Since these disturbances are not the energy. carrying waves, they will be ignored in further considerations of impedance.

3. Reflection and transformations of impedance

It follows from (1.11) that the determination of the acoustic field inside the wave-guide is now reduced to the problem of explicit calculation of the coefficients of reflection and transformation of the incident wave. According to paper [6] these coefficients have the following form:

reflection coefficient

$$R_0 = \frac{L_+(\varkappa)}{L_-(\varkappa)}; \tag{2.1}$$

transformation coefficient

$$R_n = \frac{2\varkappa L_+(\varkappa)}{(\varkappa^2-\mu_n^2)L'_-(\gamma_n)}. \tag{2.2}$$

The factors $L_+(w)$ and $L_-(w)$ are defined as

$$L_+(w) = \frac{i\sqrt{a}}{\sqrt{\varkappa+w}}\psi_+(w), \tag{2.3}$$

$$L_-(w) = \frac{i\sqrt{a}}{\sqrt{\varkappa-w}}\psi_-(w), \tag{2.4}$$

where

$$\psi_+(w) = \sqrt{\pi(\varkappa+w)H_1^{(1)}(v)J_1(v)\prod_{i=1}^{N}\frac{\gamma_i+w}{\gamma_i-w}}\,e^{S(w)/2}, \tag{2.5}$$

$$\psi_-(w) = \sqrt{\pi(\varkappa-w)H_1^{(1)}(v)J_1(v)\prod_{i=1}^{N}\frac{\gamma_i-w}{\gamma_i+w}}\,e^{-S(w)/2}, \tag{2.6}$$

N is an index of the highest mode capable of propagating freely in the wave-guide (cf. (1.17)), $S(w)$ is the complex function

$$S(w) = X(w)+iY(w). \tag{2.7}$$

For real values of w that satisfy inequality $|w| \leqslant \varkappa$ the real and imaginary parts of the function $S(w)$ equal respectively to

$$X(w) = \frac{1}{\pi}\int_{-\varkappa}^{\varkappa}\frac{\Omega(v)\,dw'}{w'-w}, \tag{2.8}$$

$$\psi(w) = \frac{2w}{\pi} - \Omega(V) + \frac{1}{i}\lim_{M\to\infty}\left[\sum_{n=N+1}^{M}\ln\frac{\gamma_n+w}{\gamma_n-w} - \frac{1}{\pi}\int_{-\gamma_M}^{\gamma_M}\frac{\Omega(v')\,dw'}{w'-w}\right]. \tag{2.9}$$

$\Omega(v)$ is the argument of Hankel function of the first kind of the first order increased by $\pi/2$:

$$\Omega(v) = \operatorname{Arg}H_1^{(1)}(v)+\frac{\pi}{2} = \operatorname{arctg}\frac{N_1(v)}{I_1(v)}+\frac{\pi}{2}. \tag{2.10}$$

Substituting (2.3) and (2.4) into (2.1) and making use of (2.5) and (2.6) we get expression for the reflection coefficient of plane wave:

$$R_0 = -\prod_{i=1}^{N}\frac{\gamma_i+\varkappa}{\gamma_i-\varkappa}\,e^{S(\varkappa)}. \tag{2.11}$$

The calculation of the transformation coefficients R_n is a little more complicated, primarily because of the occurrence of the derivative of the function $L_-(w)$ in the denominator of formula (2.2). The derivative of the function $L_-(w)$ in (2.4) equals

$$L'_-(w) = \frac{i\sqrt{a}}{\sqrt{\varkappa - w}}\left[\frac{1}{2(\varkappa - w)} + \frac{\psi'_-(w)}{\psi_-(w)}\right]\psi_-(w), \tag{2.12}$$

where the second component in brackets can be calculated by means of the logarithmic derivative [6]:

$$\frac{\psi'_-(W)}{\psi_-(W)} = -\frac{1}{2(\varkappa - w)} + \sum_{i=1}^{\infty}\int_{\gamma_{i-1}}^{\gamma_i}\frac{d\Omega(v')}{dw'}\frac{dw'}{w'-w} + \sum_{i=1}^{\infty}\frac{1}{w-\gamma_i}. \tag{2.13}$$

At the point $w = \gamma_n$, in which the function $\psi_-(w)$ vanishes, its logarithmic derivative assumes an indefinite value. Hence, $L'_-(w)$ will exist in the sense of a limit. Direct calculation leads to the following expression:

$$L'_-(\gamma_n) = -i\frac{\sqrt{a}}{\mu_n}\sqrt{-i\prod_{\substack{i=1\\ i\neq n}}^{N}\frac{\gamma_i - \gamma_n}{\gamma_i + \gamma_n}}\cdot e^{-S(\gamma_n)/2}. \tag{2.14}$$

On the other hand, the factor $L_+(\varkappa)$ in the nominator of (2.2) can be written as

$$L_+(\varkappa) = i\sqrt{a}\sqrt{-i\prod_{i=1}^{N}\frac{\gamma_i + \varkappa}{\gamma_i - \varkappa}}\, e^{S(\varkappa)/2}, \tag{2.15}$$

where use was made of the asymptotic formulae for the special functions at small values of the argument [9]:

$$\begin{aligned} J_k(v) &= \frac{1}{\Gamma(k+1)}\left(\frac{v}{2}\right)^k, \\ N_k(v) &= -\frac{\Gamma(k)}{\pi}\left(\frac{2}{v}\right)^k. \end{aligned} \tag{2.16}$$

Finally, we can write the expression for the transformation coefficient of plane wave into the n-th wave mode

$$R_n = -\frac{2\varkappa}{\mu_n}\sqrt{\prod_{\substack{i=0\\ i\neq n}}^{N}\frac{\gamma_i + \gamma_n}{\gamma_i - \gamma_n}\prod_{i=1}^{N}\frac{\gamma_i + \varkappa}{\gamma_i - \varkappa}}\; e^{[S(\gamma_n)+S(\varkappa)]/2}. \tag{2.17}$$

Effective calculations of the values of coefficients as functions of diffraction parameter are only possible by numerical methods, since the integrals in the definition of the function $S(w)$ cannot be expressed by analytic functions.

The graphs in Figs. 1 and 2 represent respectively the moduli and phases of the reflection coefficient R_0 and the transformation coefficients R_n of plane wave for all the allowed wave modes because of their values within the range [0,20] except for R_6 appearing as late as for $\varkappa = 19.62$. Numerical computations have been made starting from the point $\varkappa = 0$ with a step 0.1.

In the calculations use has been made of the generally accepted definition of modulus and phase of wave reflection coefficient

$$R_n = -|R_n| e^{i\vartheta_n}. \tag{2.18}$$

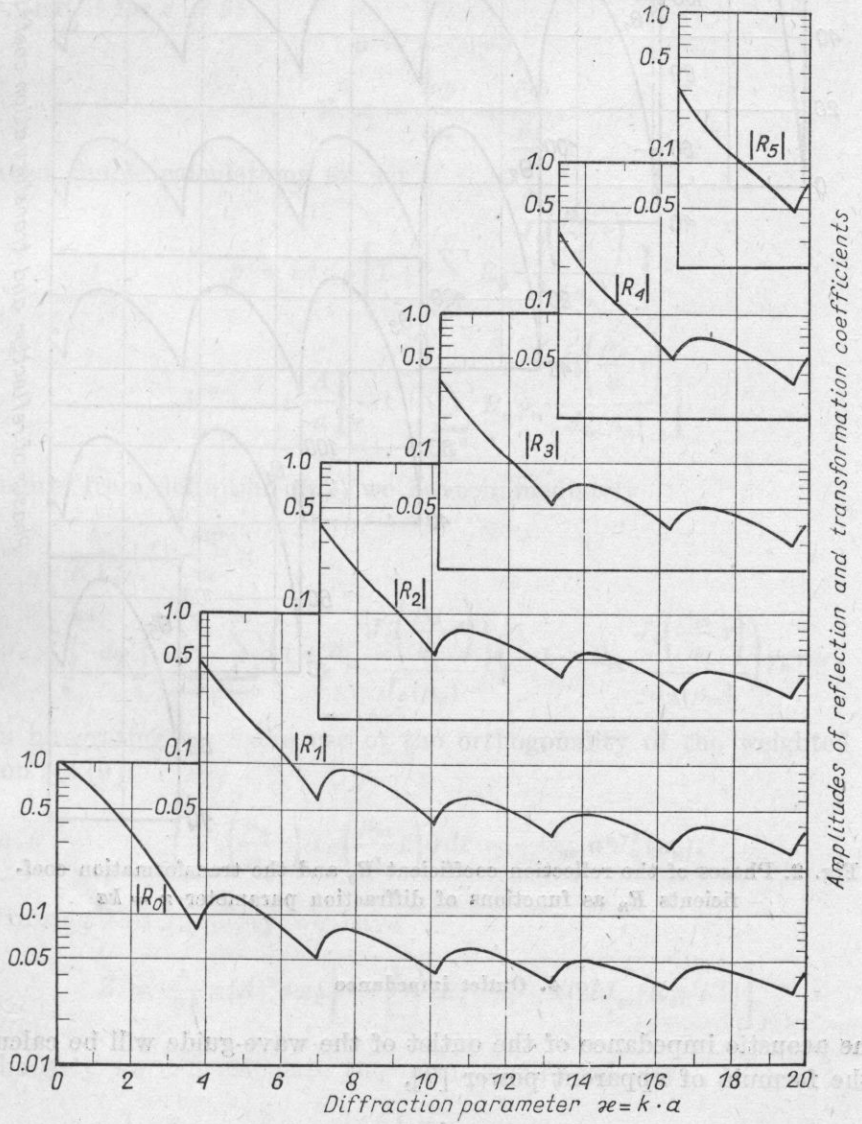

Fig. 1. Moduli of the reflection coefficient R_0 and the transformation coefficients R_n as functions of diffraction parameter $\varkappa = ka$

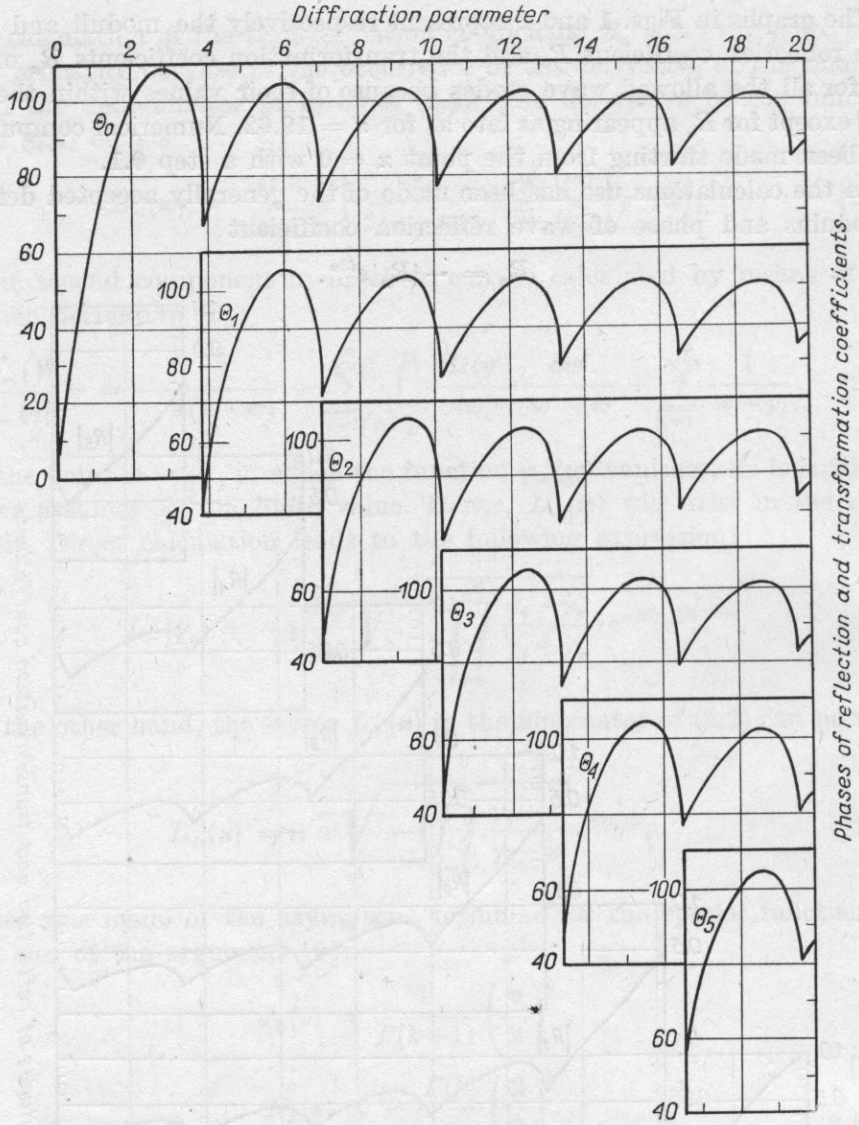

Fig. 2. Phases of the reflection coefficient R_0 and the transformation coefficients R_n as functions of diffraction parameter $\varkappa = ka$

4. Outlet impedance

The acoustic impedance of the outlet of the wave-guide will be calculated from the formula of apparent power [8],

$$P = \int_K V^* p \, d\sigma, \tag{3.1}$$

where k is the surface of the outlet, V – normal component of the velocity of vibrations, p – acoustic pressure.

The required impedance is related to the apparent power by the formula

$$Z = \frac{1}{KV_0^2} P, \tag{3.2}$$

where V_0 is the mean square of the velocity at the outlet. Knowing the acoustic potential, we can calculate the acoustic pressure and normal velocity at the outlet, that is for $z = 0$:

$$p = -i\omega\varrho\Phi, \tag{3.3}$$

$$V = -\frac{\partial\Phi}{\partial n} = \frac{\partial\Phi}{\partial z}. \tag{3.4}$$

After simple calculations we get

$$p = iA\omega\varrho\left[1 + \sum_{n=0}^{\infty} R_n \frac{J_0\left(\frac{\mu_n}{a} r\right)}{J_0(\mu_n)},\right] \tag{3.5}$$

$$V = -i\frac{A}{a}\left[-1 + \sum_{n=0}^{\infty} R_n \gamma_n \frac{J_0\left(\frac{\mu_n}{a} r\right)}{J_0(\mu_n)}\right]. \tag{3.6}$$

Hence, from definition (3.2) we have immediately

$$Z = -\frac{1}{KV_0^2}|A|^2 \frac{\omega\varrho}{a} \times$$
$$\times \int_0^{2\pi} d\varphi \int_0^a \sum_{n=0}^{\infty}\sum_{m=0}^{\infty}\left(1 + R_n \frac{J_0\left(\frac{\mu_n}{a} r\right)}{J_0(\mu_n)}\right)\left(-1 + R_m \frac{J_0\left(\frac{\mu_m}{a} r\right)}{J_0(\mu_m)}\right)\gamma_m r dr. \tag{3.7}$$

In integrating we make use of the orthogonality of the weighted Bessel function set [9]:

$$\int_0^a I_0\left(\frac{\mu_n}{a} r\right) I_0\left(\frac{\mu_m}{a} r\right) r dr = \frac{1}{2}\delta_{nm} a^2 J_0^2(\mu_n). \tag{3.8}$$

Utilizing this property we have

$$Z = \frac{1}{V_0^2}\pi|A|^2 a\omega\varrho\left[-\sum_{n=0}^{\infty}|R_n|^2\gamma_n^* + \varkappa\left(2iJ_m(R_0)+1\right)\right]. \tag{3.9}$$

Similarly we can calculate the mean square velocity

$$V_0^2 = \frac{1}{K}\int_K VV^* d\sigma = \pi\frac{|A|^2}{a^2}\left[\sum_{n=0}^{\infty}|R_n|^2|\gamma_n|^2 + \varkappa^2\left(1 - 2\,\mathrm{Re}\,(R_0)\right)\right]. \tag{3.10}$$

Acoustical impedance at the outlet is thus equal to

$$Z = \omega\varrho a \frac{\sum_{n=0}^{\infty} -\gamma_n^* |R_n|^2 + \varkappa\left(2i\,\mathrm{Im}(R_0)+1\right)}{\sum_{n=0}^{\infty} |R_n|^2 |\gamma_n|^2 + \varkappa\left(1-2\,\mathrm{Re}(R_0)\right)}. \tag{3.11}$$

We now separate the real and imaginary part of the impedance.

If N is the highest index of the wave for which n is a real number, then we have equalities

$$\gamma_n = \begin{cases} \gamma_n^*, & \text{when } n \leqslant N, \\ -\gamma_n^*, & \text{when } n > N, \end{cases}$$

and this leads to the following expressions for the real and imaginary parts of the impedance referred to the a specific impedance of environment:

$$\mathrm{Re}(Z) = \varkappa \frac{-\sum_{n=0}^{N} \gamma_n |R_n|^2 + \varkappa}{\sum_{n=0}^{\infty} |R_n|^2 |\gamma_n|^2 + \varkappa^2\left(1-2\,\mathrm{Re}(R_0)\right)}, \tag{3.12}$$

$$\mathrm{Im}(Z) = \varkappa \frac{\sum_{n=N+1}^{\infty} |\gamma_n| |R_n|^2 + 2\varkappa\,\mathrm{Im}(R_0)}{\sum_{n=0}^{\infty} |R_n|^2 |\gamma_n|^2 + \varkappa^2\left(1-2\,\mathrm{Re}(R_0)\right)}. \tag{3.13}$$

According to the remark concluding section 2, we can neglect the components of sums with an index $n > N$. Thus we finally get

$$\mathrm{Re}(Z) = \varkappa \frac{\varkappa - \sum_{n=0}^{N} \gamma_n |R_n|^2}{\sum_{n=0}^{N} |R_n|^2 |\gamma_n|^2 + \varkappa^2\left(1-2\,\mathrm{Re}(R_0)\right)}, \tag{3.14}$$

$$\mathrm{Im}(Z) = \frac{2\varkappa^2\,\mathrm{Im}(R_0)}{\sum_{n=0}^{N} |R_n|^2 |\gamma_n|^2 + \varkappa^2\left(1-2\,\mathrm{Re}(R_0)\right)}. \tag{3.15}$$

Putting $N = 0$ in (3.14) and (3.15), we shall confine ourselves to the case considered in [1], where it has been assumed that only the plane wave is reflected from the outlet and the wave modes of higher orders have been neglected.

Then these formulae take the well-known form of the expression for impedance

$$Z_0 = \frac{1+R_0}{1-R_0}. \tag{3.16}$$

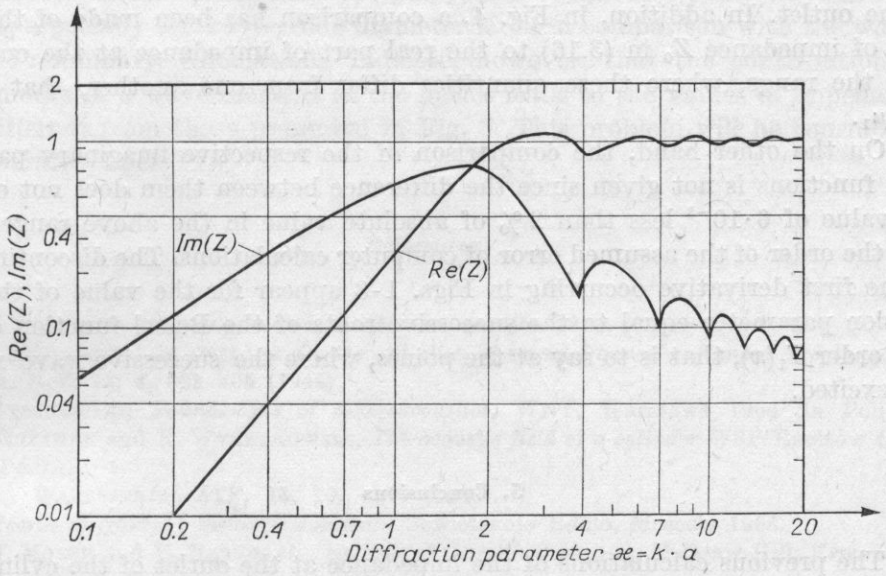

Fig. 3. The diagrams of the real and imaginary parts of the impedance at the outlet of semi-infinitive cylindrical wave-guide without baffle

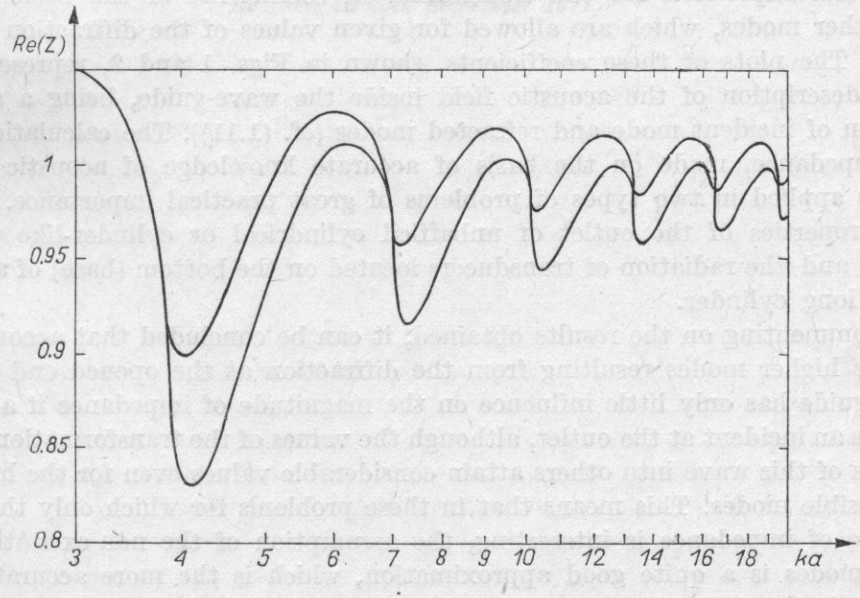

Fig. 4. The diagrams of the real part of the impedance at the outlet of the semi-infinitive cylindrical wave-guide in the case where the higher moduli of reflected waves are taken into account and in the case where it is disregarded

Fig. 3 shows the graph of the real and imaginary parts of the impedance at the outlet. In addition, in Fig. 4, a comparison has been made of the real part of impedance Z_0 in (3.16) to the real part of impedance at the outlet Z over the range, where these quantities differ from one another, that is for $\varkappa > \mu_1$.

On the other hand, the comparison of the respective imaginary parts of both functions is not given since the difference between them does not exceed the value of $6 \cdot 10^{-3}$ less than 2% of absolute value in the above range. This is of the order of the assumed error of computer calculations. The discontinuities of the first derivative occurring in Figs. 1-3 appear for the value of the diffraction parameter equal to the successive roots of the Bessel function of the first order $J_1(x)$, that is to say at the points, where the successive wave modes are excited.

5. Conclusions

The previous calculations of the impedance at the outlet of the cylindrical wave-guide, excited by the basic mode, did not account for the appearance of higher wave modes due to the phenomena occurring at the open end of the wave-guide. The application of the factorization in solving the wave equation and further development of the Wajnsztejn theory [6] permitted us to obtain the useful expression for the transformation coefficients of the basic mode into other modes, which are allowed for given values of the diffraction parameter. The plots of these coefficients, shown in Figs. 1 and 2, represent an exact description of the acoustic field inside the wave-guide, being a superposition of incident mode and refracted modes (cf. (1.11)). The calculations of the impedance, made on the basis of accurate knowledge of acoustic field, can be applied in two types of problems of great practical importance. They are: properties of the outlet of unbaffled cylindrical or cylinder-like wave-guides and the radiation of transducers located on the bottom (base) of a relatively long cylinder.

Commenting on the results obtained, it can be concluded that accounting for the higher modes resulting from the diffraction at the opened end of the wave-guide has only little influence on the magnitude of impedance if a plane wave is an incident at the outlet, although the values of the transformation coefficients of this wave into others attain considerable values even for the highest permissible modes. This means that in these problems for which only the magnitude of impedance is interesting, the assumption of the non-excitation of these modes is a quite good approximation, which is the more accurate the greater is the diffraction parameter of the wave-guide. However, one should keep in mind that the condition of the applicability of this approximation is the propagation of a "pure" basic mode in the direction of the outlet.

It is known that practically the generation of an ideal plane wave is very difficult, especially for wave-guide diameter large in comparison with the wavelength. Preliminary calculations indicate, however, that the contribution of higher modes in a wave incident at the outlet leads to the values of impedance quite different from those presented in Fig. 3. This problem will be considered in a separate paper.

References

[1] Lord RAYLEIGH, *Theory of sound*, MacMillan, London 1929.
[2] H. LEVINE and J. SCHWINGER, *On the radiation of sound from an unflanged circular pipe*, Phys. Rev. **73**, 4, 383-406 (1948).
[3] Z. ŻYSZKOWSKI, *Foundations of electroacoustics*, WNT, Warszawa 1966 (in Polish).
[4] W. RDZANEK and R. WYRZYKOWSKI, *The acoustic field of a cylinder* WSP Rzeszów 1975 (in Polish).
[5] L. A. WAJNSZTEJN, ŻTF, **18**, 10, 1543 (1948).
[6] — *Teoria diffrakcji i metod faktorizacji*, Sowietskoje Radio, Moscow 1966.
[7] P. M. MORSE and H. FESHBACH, *Methods of theoretical physics*, McGraw-Hill, New York 1953, chap. 8. 5.
[8] E. SKUDRZYK, *Die Grundlagen der Akustik*, Springer Verlag, Wien 1964.
[9] G. N. WATSON, *A treatise on the theory of Bessel functions*, Cambridge University Press, London 1946.

Received on 20th September 1977

C H R O N I C L E

7-TH WINTER SCHOOL ON MOLECULAR AND QUANTUM ACOUSTICS AND SONOCHEMISTRY

Ustronie — Brzegi, February 1978

The seventh Winter School on Molecular and Quantum Acoustics and Sonochemistry, organized by the Institute of Physics of Silesian Technical University in Gliwice and the Molecular and Quantum Physics Section of the Polish Acoustical Society with the participation of the coordinator of the interdisciplinary problem MR.I.24, was held on February 21-26, 1978, at Ustronie-Brzegi. Dr. Stanisław Szyma (Institute of Physics, Silesian Technical University in Gliwice) was the chairman of the Organizing Committee.

The School was attended by some 60 participants, i.e. twice as many as last year. They came from over 10 national scientific centres, sponsored by the Polish Academy of Sciences, the Ministry of Higher Education and Technology and by other ministries. Six sessions were held at which 37 lectures and reports were delivered giving a general description of investigations carried out in Poland in the field of quantum acoustics, acoustoelectronics and acoustooptics, ultrasound spectroscopy and sonochemistry and providing the information on the current trends in the world science. In comparison with the last year there could be observed a growing interest in the problems of acoustooptics and quantum acoustics.

List of lectures

Session 1 (Chairman prof. A. Śliwiński, Institute of Physics, Gdańsk University)

B. Zapiór — Molecular acoustics and modern sonochemistry.

A. Juszkiewicz — Investigations of the hydration of electrolytes and nonelectrolytes with the aid of the "sing around" method of the measurement of the velocity of ultrasound.

R. Płowiec — Comparison of rheological properties of mineral and synthetic oils by acoustical methods.

Z. Kaczkowski — Influence of the magnetic polarization on the piezomagnetic impedance of the water loaded alfer transducers.

Z. Toczyski — Measurements of acoustic velocities in ultrasonic wave-guides.

Session 2(Chairman prof. J. Ranachowski, Institute of Fundamental Technological Research, Polish Academy of Sciences)

L. Opilska, A. Opilski — The determination of the energy gaps in semiconductors by acoustic method.

J. Finak, A. Krzemiński — Technology of thin-film ZnO based transducers at gigahertz frequencies.

M. Szalewski — Excitation of surface waves with the aid of diffusion transducers and investigations of convolution using LiNb 03 and Li J 03 crystals.

P. Kiermasz — The technology and properties of SbSY ceramics.

W. Pajewski — Properties of transverse surface waves.

T. Pustelny – Technology of the preparation of the semiconductor-piezoelectric system and investigations of electron – phonon interaction.

P. Kwiek, A. Śliwiński, J. Wojciechowski – Use of the holographic interferometry for the investigation of the characteristics of transducer radiation.

M. Aleksiejuk, M. M. Dobrzański – Electron – phonon interaction at gigahertz frequencies.

G. Gackowska – Measurements of the distribution of the field of surface waves on SiO_2 $LiNb\ O_3$ crystals using laser and electrostatic probe.

Session 3 (Chairman prof. W. Pajewski, Institute of Fundamental Technological Research, Polish Academy of Sciences)

M. Szustakowski – Acoustooptical devices in integrated optics.

A. Byszewski – Measurements of acoustic parameters of surface waves using optical methods.

M. Drzewiecka – The visualization of acoustic surface wave.

J. Frydrychowicz – The application of X-ray methods to the diagnostics of acoustic field.

J. Merta – Acoustooptical light modulator for the synchronous modulation of the quality factor of laser resonator.

R. Leć – The elastooptical effect in $Li\ J\ O_3$ crystals.

J. Filipiak – Analysis of the interdigital transducer of acoustic surface waves.

J. Ostrowski – The surface wave resonator.

Session 4 (Chairman prof. B. Zapiór, Institute of Chemistry, Jagellonian University)

Z. Kleszczewski – Application of acoustooptical interaction for the investigation of the elasticity of non-linear crystals.

J. Berdowski, M. Strozik – The analysis of the field of acoustic surface wave using the method of the point deflection of light.

Z. Cerowski, A. Opilski – The effect of transverse drift field on the propagation of a surface wave in the piezoelectric semiconductor system.

Z. Kubik, J. Kapryan, M. Burek – Investigations of the acoustoelectric effect in the piezoelectric semiconductor system.

M. Urbańczyk – The acoustic resonator of the Raleigh surface wave.

M. Błahut – The application of Green's function theory to the investigation of the crystal lattice of thin films.

R. Bukowski – The effect of point defects on the propagation of ultrasonic waves.

Z. Jagodziński – Side sonar-properties and investigation of a model.

Session 5 (Chairman dr R. Plowiec, Institute of Fundamental Technological Research, Polish Academy of Sciences)

A. Śliwiński – Some investigations carried out in the Institute of Physics, Gdańsk University, in the field of molecular acoustics.

P. Kwiek – Experimental corroboration of Leroy's theory of light diffraction on two parallel ultrasonic beams in liquid.

C. Lewa – Rotational phase transitions in liquids.

J. Krzak – Röntgenograms of liquids, the interaction potential in the light of new trends.

R. Respondowski – On the so-called nonlinear factor in the theory of liquids.

W. Szachnowski – Standardization of measurement ressels operating in the "sing around" systems.

S. Szyma – On the possibility of increasing the accuracy of results of the analysis of acoustic sedimentation curve.

Session 6 (Chairman prof. A. Opilski, Institute of Physics, Silesian Technical University, Gliwice)

A. Filipczyńska – Wave propagation along the surface of a solid and liquid.

J. Łoziński – Investigations of the dynamic distribution of thermal emission in polycarbonate during ultrasonic welding.

P. Miecznik – Ultrasonic and hypersonic investigation of the oscillating relaxation in liquid thiophene.

K. Kunert – Ultrasonic investigations of the cross-linked polyethylene.

According to the postulate advanced during the session held in 1977, a seminar acceptance of papers presented under the subject "Quantum acoustics and acoustoelectronics" for the interdisciplinary problem MR.I.24 took place on the second day of the School to evaluate the subject matter of papers.

On the fourth day the 2-nd general meeting of the Molecular and Quantum Acoustics, Section of the Polish Acoustical Society, took place under the chairmanship of its president prof. A. Opilski (Institute of Physics, Silesium Technical University, Gliwice). At this meeting the growing importance of the Winter School was stressed and problems arising from this discussed. A twofold increase of the number of participants, as well as a substantial increase of the number of papers submitted (64% more than last year) set before the Organizing Committee a new and difficult task. A demand was put forward to increase the number of lectures to be delivered by outstanding specialists (including also those from abroad) at the expense of the number and duration of the reports

Also the proposal was presented of the coordinator of the problem MR.I.24 concerning the publication in print of more interesting and already complete materials, especially those which are the result of works realized in the frames of this problem. On the same day the participants made an excursion to Gliwice, where they acquainted themselves with the scientific and research activities of the Institute of Physics of the Silesian Technical University.

According to the opinion of the participants, the 7-th Winter School was at a good scientific level. The possibility of stimulating direct discussion and consultations in the couloirs was of great value. The Organizing Committee managed to ensure a friendly and even cordial climate which contributed to the establishment of close intellectual contacts and the exchange of views. As the seminar activities were held in the afternoon, this enabled the participants of the School to enjoy sun-bath and skiing while the daily portion of inoffensive, but apt epigrams reviewed in the shortest way the afternoon lectures.

Dr. M. M. Dobrzański